Invited Review to appear in Publ. Astron. Soc. of the Pacific
Preprint typeset using LaTeX style emulateapj

VERY HIGH ENERGY GAMMA-RAY ASTRONOMY

Michael Catanese
Department of Physics and Astronomy, Iowa State University, Ames, IA 50011-3160
Electronic mail: mcatanese@cfa.harvard.edu
and
Trevor C. Weekes
Fred Lawrence Whipple Observatory, Harvard-Smithsonian CfA, P.O. Box 97, Amado, AZ 85645-0097
Electronic mail: tweekes@cfa.harvard.edu
Invited Review to appear in Publ. Astron. Soc. of the Pacific

ABSTRACT

We present a review of the current status of very high energy γ-ray astronomy. The development of the atmospheric Cherenkov imaging technique for ground-based γ-ray astronomy has led to a rapid growth in the number of observatories. The detection of TeV γ-rays from Active Galactic Nuclei was unexpected and is providing new insights into the emission mechanisms in the jets. Next generation telescopes are under construction and will increase dramatically the knowledge available at this extreme end of the cosmic electromagnetic spectrum.

Subject headings: gamma rays: observations — galaxies: active — BL Lacertae objects: general — supernova remnants — pulsars: general — intergalactic medium

1. INTRODUCTION

Very high energy (VHE) γ-ray astronomy, (defined here as observations at energies above 300 GeV and below 100 TeV) became viable with the development of the atmospheric Cherenkov imaging technique which crossed the vital detection threshold with the detection of the Crab Nebula ten years ago (Weekes et al. 1989). Although at the periphery of the observable electromagnetic spectrum, the VHE band must now be considered a legitimate astronomical discipline with established sources, both steady and variable, both galactic and extragalactic, a growing number of observatories, and the promise of significant advances in detection techniques in the next few years. The confirmation of the detection of the Crab Nebula by more than eight groups over the past decade has given credibility to the existence of sources of TeV γ-rays and led to a rapid improvement in the sensitivity of ground-based γ-ray detection techniques.

The challenge therefore in this short review, which is aimed at the general astronomical community, is to convince the reader that there are viable methods of detecting γ-rays of energy 300 GeV and above from the ground, that a population of credible sources of various classes have been detected, and that these detections make a significant contribution to the astrophysics of high energy sources. Although, as we shall see later, there are plans to extend the ground-based detection techniques down to energies of 20 GeV, and there are viable air shower experiments that operate at energies of 50 TeV and above, this review will focus on observations in the 300 GeV to 30 TeV energy range; this has been the most studied energy band because it is easily accessible to the atmospheric Cherenkov imaging technique.

2. TECHNIQUES AND INSTRUMENTATION

2.1. *Space telescopes*

The physics involved in the interaction of photons with matter is well established. At energies above 10 MeV the predominant interaction is pair production in which a γ-ray is converted into an electron-positron pair in the presence of a nucleus: $E_\gamma \rightarrow m_{e^+}c^2 + m_{e^-}c^2$. The electron and positron carry information about the direction, energy and polarization of the primary γ-ray and hence detection methods focus on the observation of these secondary particles. The interaction length of photons in matter is 30 g-cm^2 and the earth's atmosphere is 1030 g-cm^2 thick, so the preferred (only) method of unambiguously detecting high energy γ-rays is from space vehicles (from balloons initially but now from satellites).

The basic elements of a space-borne γ-ray detector are therefore (1) a particle detector in which the γ-ray interacts and the resulting electron pair tracks are recorded; (2) a calorimeter in which the electrons are absorbed and their total energy recorded; (3) an anti-coincidence shield surrounding the tracking detector which registers (and rejects) the incidence of charged cosmic-ray particles (which are about 10,000 times more numerous than the γ-rays). In most of the telescopes flown to date, the tracking detector has been a spark chamber, the calorimeter a Sodium Iodide crystal and the anti-coincidence detector a thin sheet of scintillator. The resulting telescope is a sophisticated device which can unambiguously identify γ-rays, has an energy resolution of about 15%, an angular resolution of 1° and a field of view of 20° to 40° half angle. Unfortunately this sophistication does not come cheaply; the effective collection area is only a small fraction of the total telescope area so that in the largest telescope flown to date, the hugely successful Energetic Gamma Ray Experiment Telescope (EGRET) on the *Compton Gamma Ray Observatory* (*CGRO*) (Thompson et al. 1995; Hartman et al. 1999), the effective collection area was only 1,500 cm^2 (about the size of two pages of this journal!) whereas the actual physical instrument was about the size of a compact car. All of the γ-ray telescopes flown to date (the SAS-II telescope in 1973, the COS-B telescope in 1975, EGRET in 1991) have had the same functional form; the next generation space telescope, the Gamma-ray Large Area Space

Telescope (GLAST), scheduled for launch in 2005 (Gehrels & Michelson 1999) has the same general features but will use solid state detectors with a factor of 10-30 improvement in sensitivity.

The Third EGRET catalog (based on some four years of observation by EGRET) (Hartman et al. 1999) contains a listing of more than 250 sources of >100 MeV γ-rays, more than half of which are unidentified with any known astronomical object. In addition to a detailed map of the diffuse emission along the galactic plane, there is evidence for more than 100 galactic sources, a small number of which have been identified with pulsars and possibly with supernova remnants. The bulk of the sources away from the plane are extragalactic and have been identified with active galactic nuclei (AGNs), almost all of which are blazars. Some of the sources are variable indicating that the high energy γ-ray sky is a dynamic place. Many of the identified sources (pulsars, AGNs) have very flat spectra and have luminosities that peak in the high energy region of the spectrum. The EGRET sensitivity extends to 10 GeV but is limited by the calorimeter (at the highest energies the cascade from the electron-positron pair is not contained and charged particles from the cascade can reach the anti-coincidence detector, causing a veto of the event). Since the source flux almost invariably decreases as energy increases, it is only possible to extend observations by building larger telescopes. Even for a flat spectrum source (power law with differential spectral index -2.0), the power sensitivity of EGRET falls off with energy.

2.2. *Ground-based Telescopes*

The earth's atmosphere is as opaque to photons of energy >300 GeV as it is to photons in the *CGRO* range (100 keV to 30 GeV). However, at these higher energies the effects of atmospheric absorption are detectable at ground level, either as a shower of secondary particles from the resulting electromagnetic cascade or as a flash of Cherenkov light from the passage of these particles through the earth's atmosphere. As in the *CGRO* range, γ-ray observations are severely limited by the charged cosmic particle flux which gives superficially similar signals at ground-level and, for a given photon energy, is 10,000 times more numerous. It is not possible to veto out the charged cosmic-ray background with an anti-coincidence shield. As such, it might seem impossible to do γ-ray astronomy with such indirect techniques. However there are small, but significant, differences in the cascades resulting from the impact of a photon and a proton on the upper atmosphere; also the electromagnetic cascade retains the original direction of the photon to a high degree, and the spread of secondary particles and Cherenkov photons is so large so that a simple detector can have an incredible (by space-based γ-ray detector standards) collection area.

In practice the most successful detectors are atmospheric Cherenkov imaging telescopes (ACITs) which record the images of the Cherenkov light flashes and which can identify the images of electromagnetic cascades from putative sources with 99.7% efficiency (Aharonian & Akerlof 1997; Ong 1998). Originally proposed in 1977 (Weekes & Turver 1977), the technique was not demonstrated until ten years later when the Whipple Observatory 10-m reflector (Figure 1) was equipped with a primitive imaging camera and used to detect the Crab Nebula (Weekes et al. 1989). The technology was not new (arrays of fast photomultiplier tubes in the focal plane of large optical reflectors with readout through standard fast amplifiers, discriminators and analog-to-digital converters) but the technique was only fully exploited in the past decade. Compared to high energy space telescopes such as EGRET, ACITs have large collection areas (>50,000m^2) and high angular resolution ($\sim$0.1°). ACITs also have reasonably good energy resolution ($\sim 20 - 40\%$), but small fields of view (FOV) (<5°) and a background of diffuse cosmic electrons which produce electromagnetic cascades identical to those of γ-rays. ACITs also have low duty cycles (<10%) because the Cherenkov signals are faint and produced at altitudes of several kilometers, requiring cloudless, moonless skies for observations. Most of the results reported to date have been in the energy range 300 GeV to 30 TeV.

In recent years VHE γ-ray astronomy has seen two major advances: first, the development of high resolution ACITs has permitted the efficient rejection of the hadronic background, and second, the construction of arrays of ACITs has improved the measurement of the energy spectra from γ-ray sources. The first is exemplified by the Whipple Observatory 10-m telescope with more modern versions, CAT, a French telescope in Pyrenées (Barrau et al. 1998), and CANGAROO, a Japanese-Australian telescope in Woomera, Australia (Hara et al. 1993). The most significant examples of the second are HEGRA, a five telescope array of small imaging telescopes on La Palma in the Canary Islands run by an Armenian-German-Spanish collaboration (Daum et al. 1997), and the Seven Telescope Array in Utah, which is operated by a group of Japanese institutions (Aiso et al. 1997). These techniques are relatively mature and the results from contemporaneous observations of the same source with different telescopes are consistent (Protheroe et al. 1997). Vigorous observing programs are now in place at all of these facilities. A vital observing threshold has been achieved whereby both galactic and extragalactic sources have been reliably detected. Many exciting results are anticipated as more of the sky is observed with this present generation of telescopes.

The atmospheric Cherenkov imaging technique has now been adopted at a number of observatories whose properties are summarized in Table 1.

Above 30 TeV there are enough residual particles in the electromagnetic cascades that they can be detected at high mountain altitudes using arrays of particle detectors and fast wavefront timing (Ong 1998). These arrays have large collection areas (>10,000 m^2), good angular resolution ($\sim$0.5°), moderate energy resolution ($\sim$ 100%), good duty cycle (100%) and large FOV ($\sim$2 sr); however their ability to discriminate γ-rays from charged cosmic rays is severely limited. Despite the early promise of these experiments, which led to a considerable investment in their construction and operation, no verifiable detections have been reported by particle air shower arrays.

3. GALACTIC SOURCES

3.1. *The Crab Nebula*

The Crab Nebula was first detected with a 37 pixel camera on the Whipple Observatory 10-m optical reflector in 1989. This early and somewhat crude instrument yielded

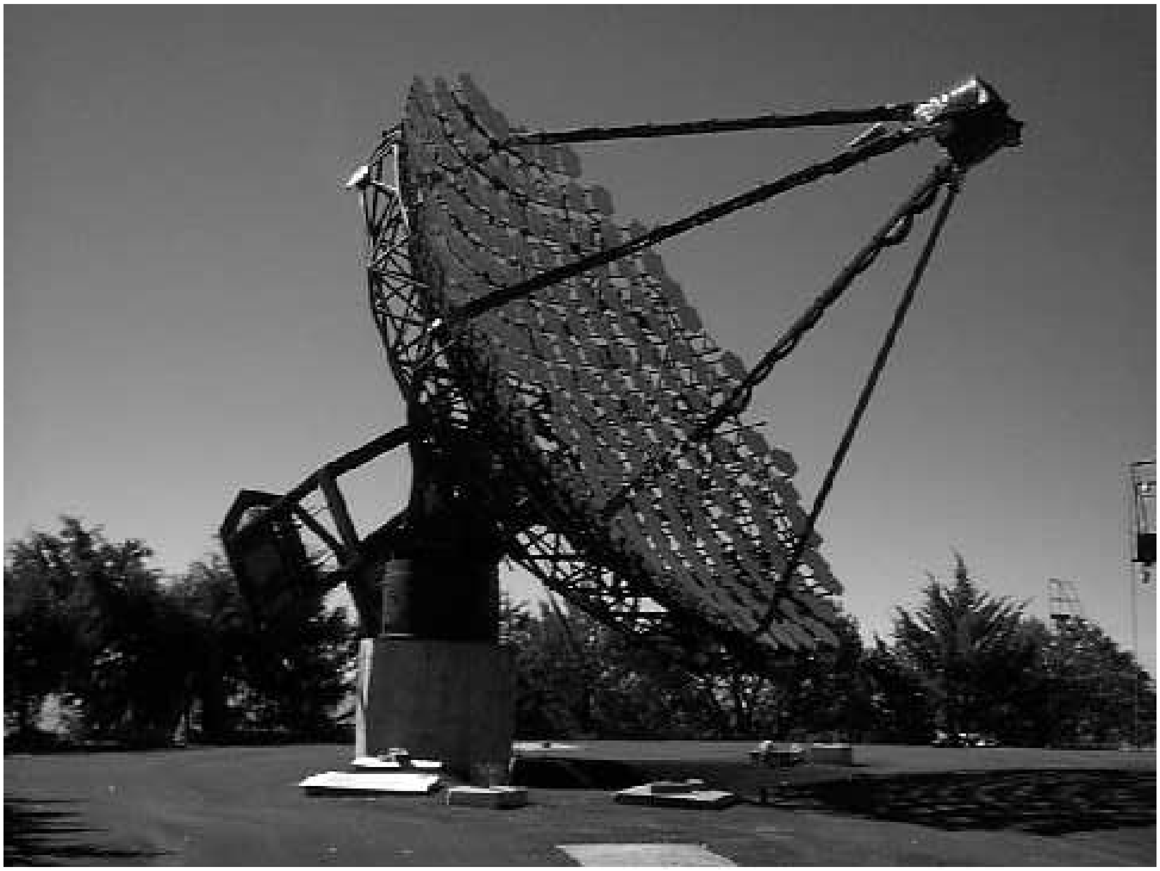

Fig. 1.— The Whipple Observatory 10-m imaging atmospheric Cherenkov telescope.

Table 1
Operating ACIT Observatories c. 1999 May

Group	Countries	Location	Telescope(s) Number×Aperture	Camera Pixels	Threshold (TeV)	Epoch Beginning
Whipple	USA-UK-Irel.	Arizona,USA	10 m	331	250	1984
Crimea	Ukraine	Crimea	6×2.4 m	6×37	1	1985
SHALON	Russia	Tien Shen, Russia	4 m	244	1.0	1994
CANGAROO	Japan-Aust.	Woomera,Aust.	3.8 m	256	0.5	1994
HEGRA	German-Armen.-Sp.	La Palma, Sp.	5×3 m	5×271	0.5	1994
CAT	France	Pyrenées	3 m	600	0.25	1996
Durham	UK	Narrabri,Aust.	3×7 m	1×109	0.25	1996
TACTIC	India	Mt.Abu,India	10 m	349	0.3	1997
Seven TA	Japan	Utah,USA	7×2 m	7×256	0.5	1998

a $9\,\sigma$ detection with some 60 hours of integration on the source (Weekes et al. 1989). The detection relied on discrimination of the γ-ray images from the much more numerous hadron background images. The possibility of a systematic effect with a new, and not yet proven, technique could not be completely discounted (although numerous tests were made for consistency). Nonetheless it required the independent confirmation of the detection by other groups using different versions of the technique to really convince skeptics. The Whipple group subsequently detected the source at the $20\,\sigma$ level using an upgraded camera (109 pixels) (Vacanti et al. 1991) and now routinely detects the source at the 5-6 σ level in an hour of observation. The detected photon rate (about 2 per minute) is more than that registered by EGRET at its optimum energy (100 MeV).

Since then the Crab has been detected by eight independent groups using different versions of the atmospheric Cherenkov imaging technique (including one group in the Southern Hemisphere). Some of these detections are listed in Table 2. The energy spectrum is now well determined at energies between 300 GeV and 50 TeV (Hillas et al. 1998;Tanimori et al. 1998b). To date there have been no positive detections reported by air shower array experiments using particle detectors (which operate at somewhat higher energies)(Ong 1998).

The simple Compton-synchrotron model (Gould 1965) has been updated to take account of a better understanding of the nebula (de Jager & Harding 1992; Hillas et al. 1998); the measured flux is in good agreement

Table 2
Flux from the Crab Nebula

Group	VHE Spectrum (10^{-11} photons cm^{-2} s^{-1})	E_{th} (TeV)
Whipple (1991)[a]	$(25(E/0.4TeV))^{-2.4\pm0.3}$	0.4
Whipple (1998)[b]	$(3.2 \pm 0.7)(E/TeV)^{(-2.49\pm0.06_{stat}\pm0.05_{syst}}$	0.3
HEGRA (1999)[c]	$(2.7 \pm 0.2 \pm 0.8)(E/TeV)^{-2.61\pm0.06_{stat}\pm0.10_{syst}}$	0.5
CAT (1998)[d]	$(2.7 \pm 0.17 \pm 0.40)(E/TeV)^{-2.57\pm0.14_{stat}\pm0.08_{syst}}$	0.25

[a]Vacanti et al. 1991
[b]Hillas et al. 1998
[c] Priv. Com.: A. Konopelko
[d] Priv. Com.: M. Punch

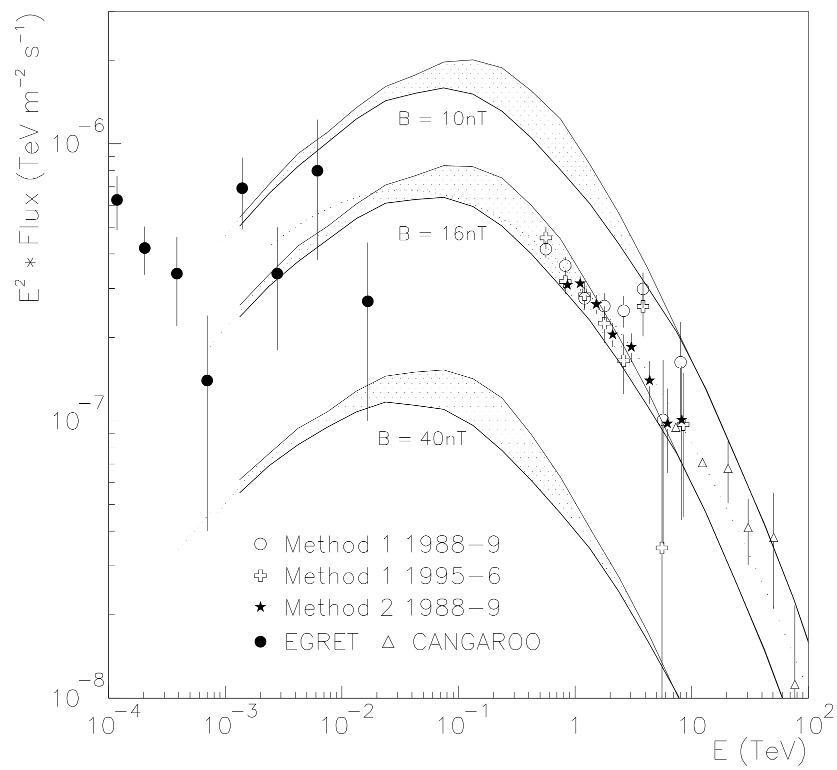

Fig. 2.— The VHE spectral energy distribution of the Crab Nebula compared with the predictions of a synchrotron self-Compton emission model (Hillas et al. 1998).

with the predicted flux for a value of magnetic field ($1.6 \pm 0.1 \times 10^{-4}$ G) that is slightly lower than the equipartition value (Figure 2). Although this model is certainly simplistic given the structure now seen in optical images of the nebula, it shows that there is a viable mechanism that must work at some level.

As in many other bands of the electromagnetic spectrum, the Crab Nebula has become the standard candle for TeV γ-ray astronomy. Most importantly perhaps it is available as a steady source to test and calibrate the ACIT and can be seen from both hemispheres. Improvements in analysis techniques developed on Crab Nebula data have led directly to the detections of the AGNs discussed below.

3.2. *Supernova Remnants: Plerions*

The Crab Nebula is a somewhat unique object and hence one could not confidently predict what other supernova remnants might be detectable. The Crab is a member of that sub-class of supernova remnants known as plerions in which a bubble of relativistic particles is powered by a central pulsar. No other plerions have been seen by telescopes in the Northern Hemisphere (Reynolds et al. 1993) (Table 3). However two have been detected in the Southern Hemisphere by the CANGAROO group. They first reported a detection of PSR1706-44 at TeV energies in 1993 (Kifune et al. 1995) based on sixty hours of observation in the summer of 1992. PSR1706-44 is identified with a pulsar (of period 102 ms) and appears to be associated with a supernova remnant, possibly a plerion. At GeV energies it has a very flat spectrum. The energy spectrum is hard with a flux above 1 TeV of about 0.15×10^{-11}-

Table 3
TeV Observations of Plerions

Source	Energy (GeV)	Flux/Upper Limit ($\times 10^{-11}$ cm^{-2} s^{-1})	Group
Crab Nebula	400	7.0	Whipple, ASGAT, HEGRA, TA Crimea, *Gamma, CANGAROO, CAT
PSR 1706-44	1000	0.8	CANGAROO, Durham
Vela	2500	0.29	CANGAROO
SS 433	550	<1.8	Whipple
3C 58	550	<1.1	Whipple
PSR 0656+14	1000	<3.4	Whipple

cm^{-2}-s^{-1}. There is no evidence that the signal is periodic. The detection has been confirmed by the University of Durham group working in Narrabri, Australia (Chadwick et al. 1997).

The CANGAROO group have also reported the detection of a 6σ signal from the vicinity of the Vela pulsar (Yoshikoshi et al. 1997). The integral γ-ray flux above 2.5 TeV is 2.5×10^{-12} photons cm^{-2} s^{-1}. Again there is no evidence for periodicity and the flux limit is about a factor of ten less than the steady flux. The signal is offset (by 0.14°) from the pulsar position which makes it more likely that the source is a synchrotron nebula. Since this offset position is coincident with the birthplace of the pulsar it is suggested that the progenitor electrons are relics of the initial supernova explosion and they have survived because the magnetic field was weak.

3.3. *Pulsars*

The power spectra of most of the γ-ray pulsars (Thompson 1997) are extremely flat with maximum power often coming in the GeV energy range (see Figure 3). Because pulsar models often involve electrons with energies up to 10^{15}eV, it would come as no surprise if TeV γ-rays should emerge from the pulsar magnetosphere and be detected. Although there is, as yet, no established model for high energy γ-ray emission from pulsars, it appears that, in general, the detection of pulsed TeV γ-rays would favor outer gap (Romani 1996) over polar cap (Daugherty & Harding 1982) models. This is because, in the latter models, the TeV γ-rays are attenuated by pair-production interactions with the intense magnetic fields near the pulsars.

Sensitive upper limits have been obtained for emission by the Crab pulsar (Lessard et al. 1999), Geminga (Akerlof et al. 1993) and the Vela pulsar (Yoshikoshi et al. 1997); in general these confirm the steepening of the spectra seen at 10 GeV energies. The radio pulsar PSR 1951+32 is particularly interesting because the power spectrum indicates that the maximum power occurs at energies of at least a few GeV (Figure 3); in the EGRET measurements there is no evidence for a high energy cutoff. In fact, the flux continues to rise with energy up to the highest energy observation. Outer gap models suggest that the pulsar should be detectable at higher energies. Observations of PSR 1951+32 by the Whipple group reported only an upper limit (Srinivasan et al. 1997). This upper limit to the pulsed flux is two orders of magnitude below the flux extrapolated from the EGRET measurements. This represents the most dramatic turn-over in the spectrum of a γ-ray pulsar and hence puts the most severe constraints on the models.

3.4. *Supernova Remnants: Shell*

Supernova remnants (SNRs) are widely believed to be the sources of hadronic cosmic rays up to energies of approximately $Z \times 10^{14}$ eV, where Z is the nuclear charge of the particle (for a review see Jones et al. 1998). The arguments in support of this statement are two-fold. First, supernova blast shocks are some of the few galactic sites capable of satisfying the energy required for the production of galactic cosmic rays, although even these must have a high efficiency, $\sim$10% − 30% (e.g., Drury, Markiewicz & Völk 1989), for converting the kinetic energy of supernova explosions into high energy particles. Second, the model of diffusive shock acceleration (e.g., Blandford & Ostriker 1978; Bell 1978; Legage & Cesarsky 1983), which provides a plausible mechanism for efficiently converting the explosion energy into accelerated particles, naturally produces a power-law spectrum of $dN/dE \propto E^{-2.1}$. This is consistent with the inferred spectral index at the source for the observed local cosmic-ray spectrum of $dN/dE \propto E^{-2.7}$, after correcting for the effects of propagation in the galaxy (e.g., Swordy et al. 1990).

The origins of cosmic rays cannot be studied directly because interstellar magnetic fields isotropize their directions, except perhaps at the highest energies ($\gtrsim 10^{18}$ eV). Thus, we must look for indirect signals of their presence from astrophysical sources. That SNRs accelerate *electrons* to high energies is well-established from observations of synchrotron emission in the shells of SNRs at radio and, more recently, X-ray (e.g., Koyama et al. 1995) wavelengths. However, it is difficult to extrapolate from these data to inferences about the nature of the acceleration of hadrons in these same objects.

Evidence of shock acceleration of hadronic cosmic rays in SNR shells could come from measurements of γ-ray emission in these objects. Collisions of cosmic-ray nuclei with the interstellar medium result in the production of neutral pions which subsequently decay into γ-rays. The γ-ray spectrum would extend from below 10 MeV up to $\sim$1/10 of the maximum proton energy ($\gtrsim$ 10 TeV), with a distinctive break in the spectrum near 100 MeV due to the resonance in the cross-section for π^0 production. As γ-ray production requires interaction of the hadronic cosmic

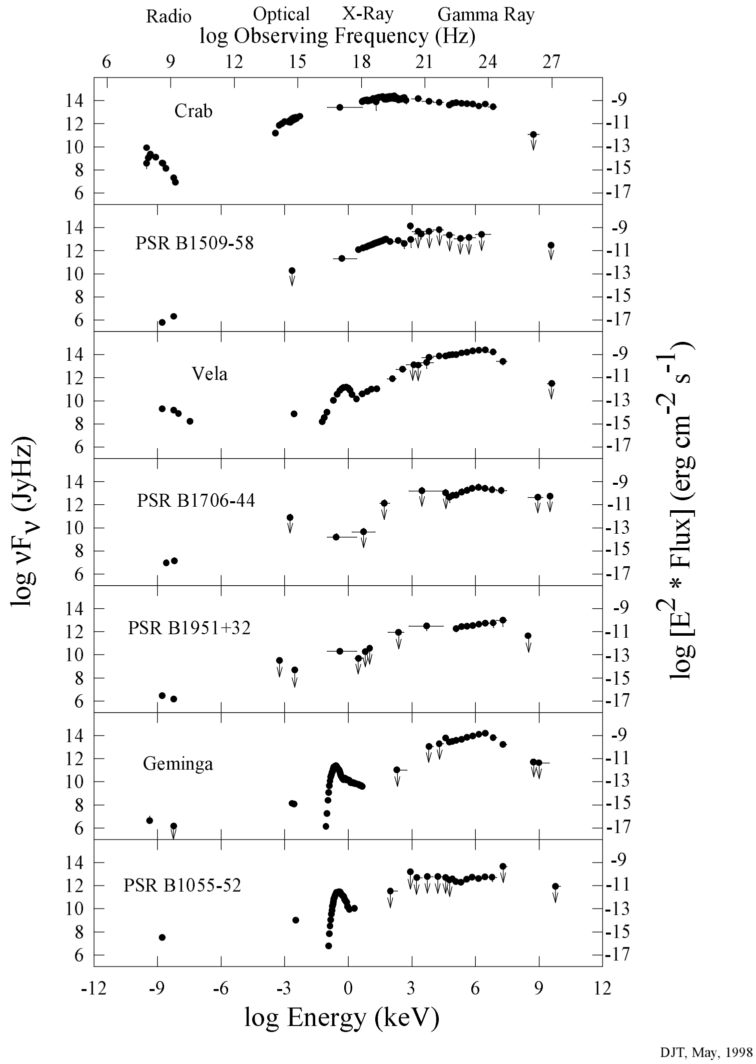

FIG. 3.— Power spectrum of γ-ray pulsars detected with EGRET (Thompson 1997).

rays with target nuclei, this emission should be stronger for those SNR located near, or interacting with, dense targets, such as molecular clouds. The cosmic-ray density, and hence the associated γ-ray luminosity, will increase with time as the SNR passes through its free expansion phase, will peak when the SNR has swept up as much interstellar material as contained in the supernova ejecta (the Sedov phase) and gradually decline thereafter (Drury, Aharonian & Völk 1994; Naito & Takahara 1994). Thus, γ-ray bright SNRs should be "middle-aged."

From the calculations of Drury et al. (1994), the luminosity of γ-rays from secondary pion production may be detectable by the current generation of satellite-based and ground-based γ-ray detectors, particularly if the objects are located in a region of relatively high density in the interstellar medium. In support of this hypothesis, EGRET has detected signals from several regions of the sky consistent with the positions of shell-type SNRs (Sturner & Dermer 1995; Esposito et al. 1996; Lamb & Macomb 1997; Jaffe et al. 1997). However, the EGRET detections alone are not sufficient to claim the presence of high energy hadronic cosmic rays. For instance, the relatively poor angular resolution of EGRET makes difficult to definitively identify the detected object with the SNR shell. Because of this, embedded pulsars (Brazier et al. 1996; de Jager & Mastichiadis 1997; Harrus, Hughes & Helfand 1996) and an X-ray binary (Kaaret et al. 1999) consistent with the positions of some of these EGRET sources have been suggested as alternative counterparts. In addition, significant background from the diffuse Galactic γ-ray emission complicates spectral measurements. To complicate matters further, with the detection of X-ray synchrotron radiation from SNR shells, the possibility that γ-rays could be produced via inverse Compton scattering of ambient soft photons has been realized (Mastichiadis & de Jager 1996; Mastichiadis 1996). Bremsstrahlung radiation may also be a significant source of γ-rays at MeV-GeV energies (de Jager & Mastichiadis 1997; Gaisser, Protheroe & Stanev 1998).

3.4.1. *VHE γ-ray observations*

Measurements of γ-rays at very high energies may help resolve the puzzle of the γ-ray emission from the EGRET-detected sources. VHE γ-ray telescopes have much better angular resolution than EGRET, reducing the source confusion associated with any detection. Also, because the diffuse Galactic γ-ray emission has a relatively steep

Table 4
Observations of shell-type supernova remnants

Object Name	Observation Time (min.)	Energy (TeV)	Integral Flux[a] (10^{-11} cm^{-2} s^{-1})	Ref.
Tycho	867.2	>0.3	<0.8	Buckley et al. 1998
IC 443[b]	1076.7	>0.3	<2.1	Buckley et al. 1998
	678.0	>0.5	<1.9[c]	Hess et al. 1997
W 44[b]	360.1	>0.3	<3.0	Buckley et al. 1998
W 51	468.0	<0.3	<3.6	Buckley et al. 1998
γ-Cygni[b]	560.0	>0.3	<2.2	Buckley et al. 1998
	2820.0	>0.5	<1.1[c]	Hess et al. 1997
W 63	140.0	>0.3	<6.4	Buckley et al. 1998
SN 1006	2040.0	>1.7	$0.46 \pm 0.6_{\rm stat} \pm 1.4_{\rm sys}$	Tanimori et al. 1998a

[a]Upper limits from Buckley et al. (1998) are at the 99.9% confidence level and those from Hess et al. (1997) are at the $3\,\sigma$ confidence level.
[b]Associated with an EGRET source.
[c]Upper limits were converted from fractions of >500 GeV Crab flux using the measured Crab flux of Hillas et al. (1998).

spectrum, $\propto$ E$^{-2.4}$ – E$^{-2.7}$ (Hunter et al. 1997), compared with the expected $\sim$ E$^{-2.1}$ spectrum of γ-rays from secondary pion decay, contamination from background γ-ray emission should be less in the VHE range. Thus, in recent years, searches for emission from shell-type SNRs have been a central part of the observation program of VHE telescopes.

The Whipple Collaboration has published the results of observations of six shell-type SNRs (IC 443, γ-Cygni, W 44, W 51, W 63, and Tycho) selected as strong γ-ray candidates based on their radio properties, distance, small angular size, and possible association with a molecular cloud (Buckley et al. 1998;Hess et al. 1997). The small angular size was made a requirement due to the limited field of view (3° diameter) of the Whipple telescope at that time. VHE telescopes can also detect fainter γ-ray sources if they are more compact, because they can reject more of the cosmic-ray background. IC 443, γ-Cygni, and W 44 are also associated with EGRET sources (Esposito et al. 1996). Despite long observations, no significant excesses were observed, and stringent limits were derived on the VHE flux (see Table 4).

In contrast to the upper limits derived by the northern hemisphere telescopes, the CANGAROO Collaboration has recently reported evidence for TeV γ-ray emission from the shell-type SNR, SN 1006 (Tanimori et al. 1998a). Observations taken in 1996 and 1997 indicate a statistically significant excess from the northeast rim of the SNR shell (see Figure 4). The position of the excess is consistent with the location of non-thermal X rays detected by the *ASCA* experiment (Koyama et al. 1995). If this object is confirmed as a TeV γ-ray source, it represents the first direct evidence of acceleration of particles to TeV energies in the shocks of SNRs.

3.4.2. *Implications of the γ-ray observations*

If the EGRET detections do indicate the presence of γ-rays produced by secondary pion decay, the measured flux can be compared with the VHE upper limits. These VHE upper limits and the EGRET measurements are compared to the predicted fluxes from the model of Drury et al. (1994) in Figure 5 (Buckley et al. 1998). The solid curves are normalized to the integral >100 MeV flux detected by EGRET assuming a source cosmic-ray spectrum of E$^{-2.1}$, so they assume that the EGRET emission is entirely due to cosmic-ray interactions and that the cosmic-ray spectrum at the source has the canonical spectrum. In the cases of γ-Cygni, IC 443, and W 44, the Whipple upper limits lie a factor of ~25, 10, and 10, respectively, below the model extrapolations and require either a spectral break or a differential source spectrum steeper than E$^{-2.5}$ for γ-Cygni and E$^{-2.4}$ for IC 443 (Buckley 1998). In addition, the measured EGRET spectra, while consistent with a spectral index of about 2, do not show the flattening of the γ-ray spectrum near 100 MeV which would be expected if the γ-rays result from secondary pion decay. Gaisser et al. (1998) performed multiwavelength fits to the EGRET and Whipple results and concluded that if the EGRET detections are truly from the shells of the SNRs, the EGRET data must be dominated at low energies by electron bremsstrahlung radiation, but the source spectrum at high energies must still be relatively steep (~E$^{-2.4}$) to account for the Whipple upper limits (cf., Buckley et al. 1998).

If, on the other hand, the >100 MeV emission results from some other emission mechanism, such as the interactions of high energy electrons accelerated by embedded pulsars or in the SNR shocks, the EGRET results should not be compared to the Whipple data. Instead, the Whipple data must be considered alone in the context of the secondary pion decay models. This possibility was also investigated by Buckley et al. (1998) and is shown by the dashed curves in Figure 5. The dashed curves represent a conservative estimate of the range of allowable parameter values for the Drury et al. (1994) model, without reference to the EGRET detections. For this comparison, there is

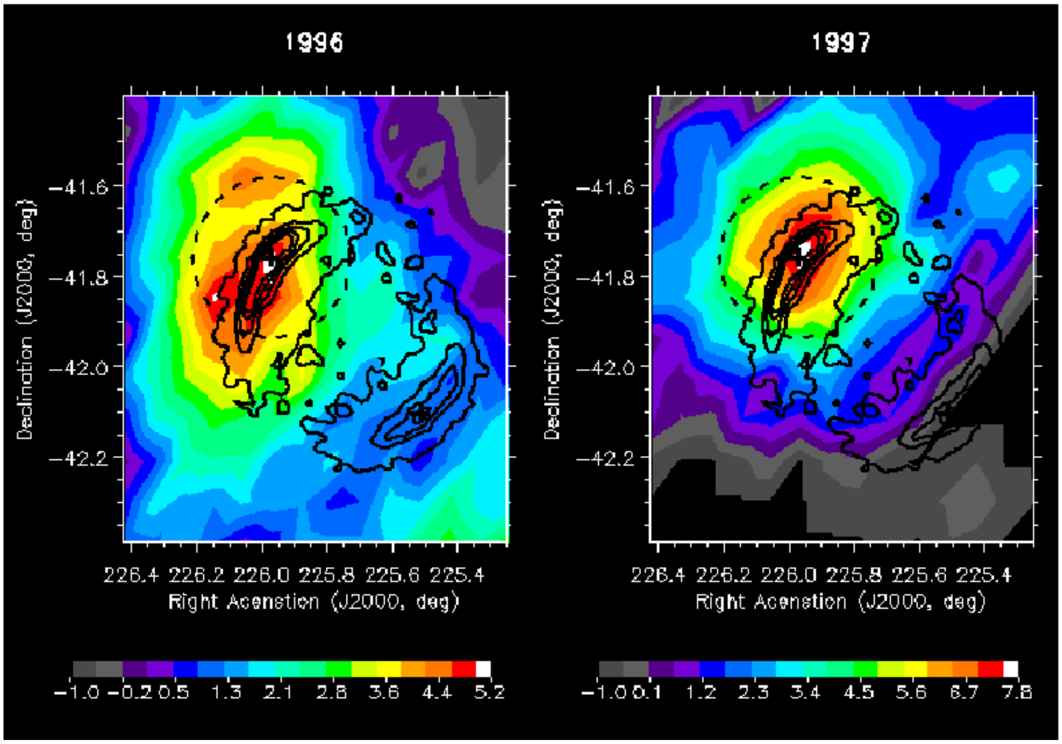

FIG. 4.— Left: contour map of the statistical significance of the excess emission from SN 1006 as observed with the CANGAROO telescope in 1996. Right: the same plot for data taken in 1997. The solid lines indicate the contour map of non-thermal X-ray emission detected with *ASCA*. The dashed circles indicate the angular resolution of the CANGAROO telescope. Figure from Tanimori et al. (1998a).

still room for the models to work in these objects. However, the upper limits in some (e.g., IC 443) are beginning to strain the limits of the available parameter space. It will take more sensitive measurements with future telescopes to fully span the allowable parameter space and see if we need to reconsider our assumptions about the sources of cosmic rays within our Galaxy.

The TeV emission from SN 1006 detected by the CANGAROO group also does not require the presence of hadronic cosmic rays. In fact, the most common explanation for the detected emission is inverse Compton scattering of electrons with cosmic microwave background photons (Reynolds 1996; Mastichiadis & de Jager 1996). The main arguments for this are that the emission is centered on one of the regions where the synchrotron emission was detected with *ASCA* and the lack of evidence for a nearby molecular cloud needed to boost the TeV γ-ray flux to a detectable level. Under the assumption that the emission is from inverse Compton scattering, Tanimori et al. (1998a) have combined their data with the *ASCA* results to derive an estimate of $6.5 \pm 2\,\mu$G for the magnetic field within the SNR shell. The observations also provide an upper limit on the acceleration time. Thus, the TeV observations provide previously unknown parameters for models of the shock acceleration in SNRs. Unfortunately, the possibility of inverse Compton emission from the shells of SNRs also confuses the issue for using γ-rays as a probe of cosmic-ray acceleration in SNRs. Future measurements will need to provide accurate spectra and spatial mapping of the γ-ray emission from SNRs in order for the source of the γ-ray emission to be unambiguously resolved.

4. EXTRAGALACTIC SOURCES

4.1. *Active Galactic Nuclei*

In recent years, high energy γ-rays have come to play an important role in the study of AGNs. Before the launch of *CGRO* in 1991, the only known extragalactic source of high energy γ-rays was 3C 273 which had been detected with the COS-B satellite 20 years ago (Swanenburg et al. 1978). The EGRET detector on the *CGRO* has identified more than 65 AGNs which emit γ-rays at energies above 100 MeV (Hartman et al. 1999), and a substantial fraction of those sources which remain unidentified in the EGRET catalog are likely to be AGNs as well. In addition, the Whipple Observatory γ-ray telescope has discovered three AGNs which emit at energies above 300 GeV (Punch et al. 1992; Quinn et al. 1996; Catanese et al. 1998) and there are recent detections of two other AGNs with Cherenkov telescopes (Chadwick et al. 1999; Neshpor et al. 1998). During flaring episodes, the γ-ray emission can greatly exceed the energy output of the AGNs at all other wavelengths. Thus, any attempt to understand the physics of these objects must include consideration of the γ-ray emission.

All of the AGNs detected in high energy γ-rays are radio-loud sources with the radio emission arising primarily from a core region rather than from lobes. These types of AGNs are often collectively referred to as “blazars,” and include BL Lacertae (BL Lac) objects, flat spectrum radio-loud quasars (FSRQs), optically violent variables, and superluminal sources. The emission characteristics of blazars include high polarization at radio and optical wavelengths, rapid variability at all wavelengths, and predominantly non-thermal emission at most wavelengths. The emission from blazars is believed to arise from relativistic

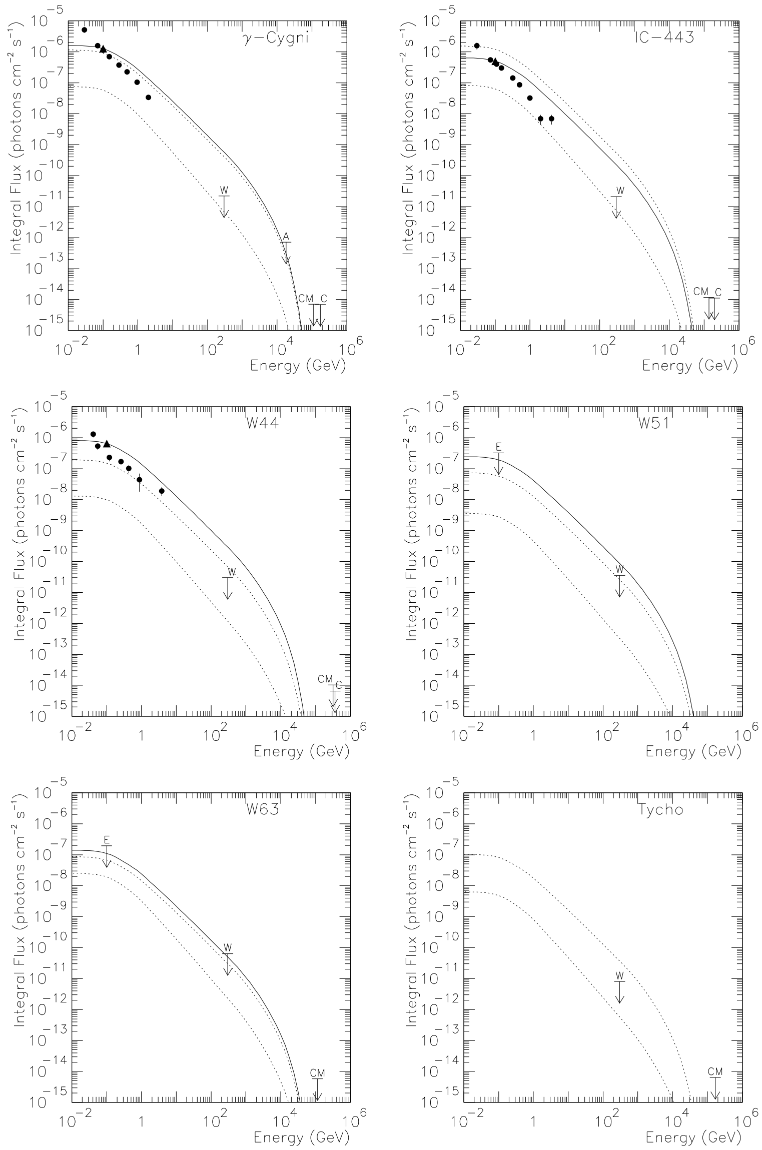

Fig. 5.— Whipple Observatory upper limits (W) shown along with EGRET integral fluxes (E) and integral spectra. Also shown are CASA-MIA upper limits (CM) from Borione et al. (1995), Cygnus upper limits (C) from Allen et al. (1995), and the AIROBICC upper limit from Prosch et al. (1996). The solid curves indicate extrapolations from the EGRET integral data points at 100 MeV (indicated by the triangles). The dashed curves are estimates of the allowable range of fluxes from the model of Drury et al. (1994). Figure from Buckley et al. (1998).

jets oriented at small angles to our line of sight. If so, the observed radiation will be strongly amplified by relativistic beaming (Blandford & Rees 1978). Direct evidence for relativistic beaming of the radio emission comes from Very Long Baseline Interferometer (VLBI) observations of apparent superluminal motion in many blazars (e.g., Vermeulen & Cohen 1994). The rapid variability and high luminosities of the detected γ-ray sources imply that the γ-rays are also beamed (see § 4.1.3).

There is a growing consensus that blazars are all the same type of object, perhaps differing only in intrinsic luminosity (e.g., Fossati et al. 1998; Ghisellini et al. 1998) or some combination of luminosity and viewing angle (e.g., Georganopoulos & Marscher 1998). However, for this work we will continue the practice of referring to BL Lac objects and FSRQs as distinct objects: BL Lac objects are those blazars which have optical emission lines with equivalent width < 5 Å and FSRQs are the remaining blazars. As we will see, this distinction may be important in explaining why only BL Lac objects are detected at very high energies.

The spectral energy distribution of blazars appears to consist of two parts. First, a low energy component exhibits a power per decade distribution that rises smoothly from radio wavelengths up to a broad peak in the range spanning infrared (IR) to X-ray wavelengths, depending on the specific blazar type, above which the power output rapidly drops off. Second, a distinct, high energy component, which does not extend smoothly from the low energy component, is often seen. It typically becomes apparent in the X-ray range and has a peak power output in the γ-ray range between ~1 MeV and 1 TeV (e.g., von Montigny et al. 1995), again depending on the specific blazar type. When plotted as $E^2 dN/dE$ (or equivalently νF_ν) the

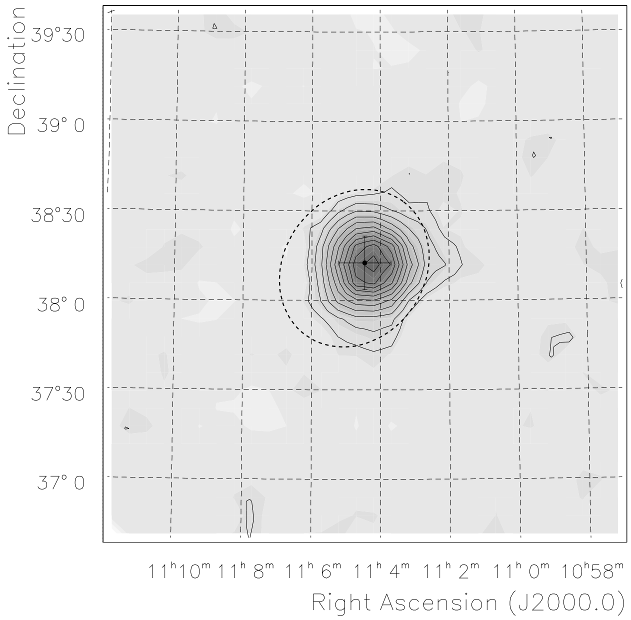

Fig. 6.— Two-dimensional plot of the VHE γ-ray emission from the region around Mrk 421. The gray scale is proportional to the number of excess γ-rays and the solid contours correspond to $2\,\sigma$ levels. The dashed ellipse give the 95% confidence interval determined by EGRET (Thompson et al. 1995). The position of Mrk 421 is indicated by the cross. Figure from Buckley et al. (1996).

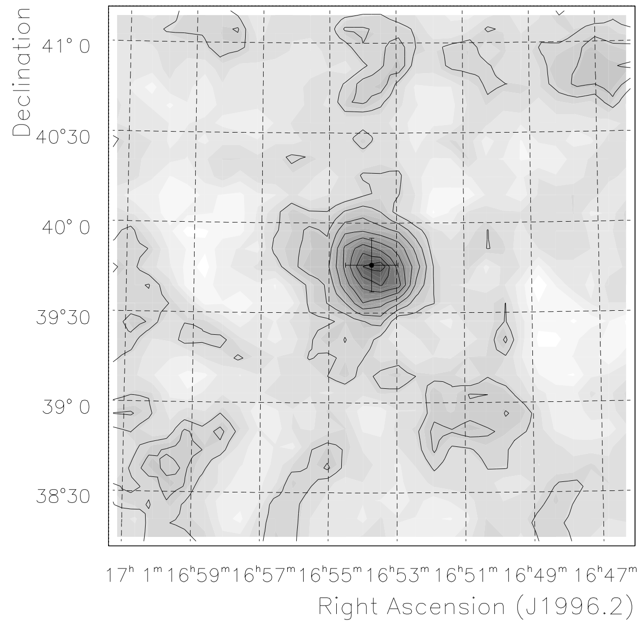

Fig. 7.— Two-dimensional plot of the VHE γ-ray emission from the region around Mrk 501. The gray scale is proportional to the number of excess γ-rays and the solid contours correspond to $1\,\sigma$ levels. The position of Mrk 501 is indicated by the cross.

spectral energy distribution shows a two-humped shape, though some objects show evidence of a third component (e.g., Kubo et al. 1998).

Though there is no general consensus on the origin of these emission components, it is generally agreed that the low energy component arises from incoherent synchrotron emission by relativistic electrons within the jet (e.g., Blandford & Rees 1978). This is supported most strongly by the high-level, variable polarization observed in these objects at radio and optical wavelengths. The origin of the high energy emission is a matter of great interest. There are many variations of the models and here we only briefly mention a few which are most often invoked to explain the γ-ray emission. The most popular models at this time are those in which the γ-rays are produced through inverse Compton scattering of low energy photons by the same electrons which produce the synchrotron emission at lower energies. Synchrotron self-Compton (SSC) emission (e.g., Königl 1981; Maraschi et al. 1992; Bloom & Marscher 1996), in which the seed photons for the scattering are the synchrotron photons already present in the jet, must occur at some level in all blazars, but models in which the γ-ray emission arises predominantly from inverse Compton scattering of seed photons which arise outside of the jet, either directly from an accretion disk (Dermer, Schlickeiser & Mastichiadis 1992) or after being re-processed in the broad-line region or scattering off thermal plasma (Sikora, Begelman & Rees 1994), appear to fit the observations satisfactorily as well. Another set of models proposes that the γ-rays are produced by proton-initiated cascades (e.g., Mannheim 1993). As we will show in §4.1.3, the γ-ray observations strain both types of models, but do not, at present, rule any out.

In the remainder of this section we discuss the status of VHE observations and the emission characteristics of the detected objects (§4.1.1), the results of multi-wavelength campaigns on the detected objects (§4.1.2) which are the best probe of the physics of blazars, and finally briefly discuss some of the implications of these observations on our understanding of the physics of the blazars and on the models which purport to explain them.

4.1.1. *Observational Status and Emission Characteristics*

The BL Lac object Markarian 421 (Mrk 421, $z = 0.031$) was detected as the first extragalactic source of VHE γ-rays in 1992 using the Whipple Observatory γ-ray telescope (Punch et al. 1992). A two-dimensional image of the emission from Mrk 421 is shown in Figure 6. Although Mrk 421 had previously been part of an active program of observing extragalactic sources (Cawley et al. 1985) by the Whipple Collaboration, the observations which led to the detection of Mrk 421 at TeV energies were initiated in response to the detection of several AGN by the EGRET experiment. The initial detection indicated a $6\,\sigma$ excess and the flux above 500 GeV was approximately 30% of the flux of the Crab Nebula at those energies. Mrk 421 has been confirmed as a source of VHE γ-rays by the HEGRA Collaboration (Petry et al. 1996), the Telescope Array Project (Aiso et al. 1997), and the SHALON telescope (Sinitsyna et al. 1997) and, as discussed in § 4.1.2 below, multi-wavelength correlations have confirmed that the VHE source is indeed Mrk 421 and not some other object.

With the successful detection of Mrk 421, the Whipple Collaboration initiated a search for VHE emission from several other blazar-type AGNs, concentrating at first on those objects detected by EGRET, but also spending a

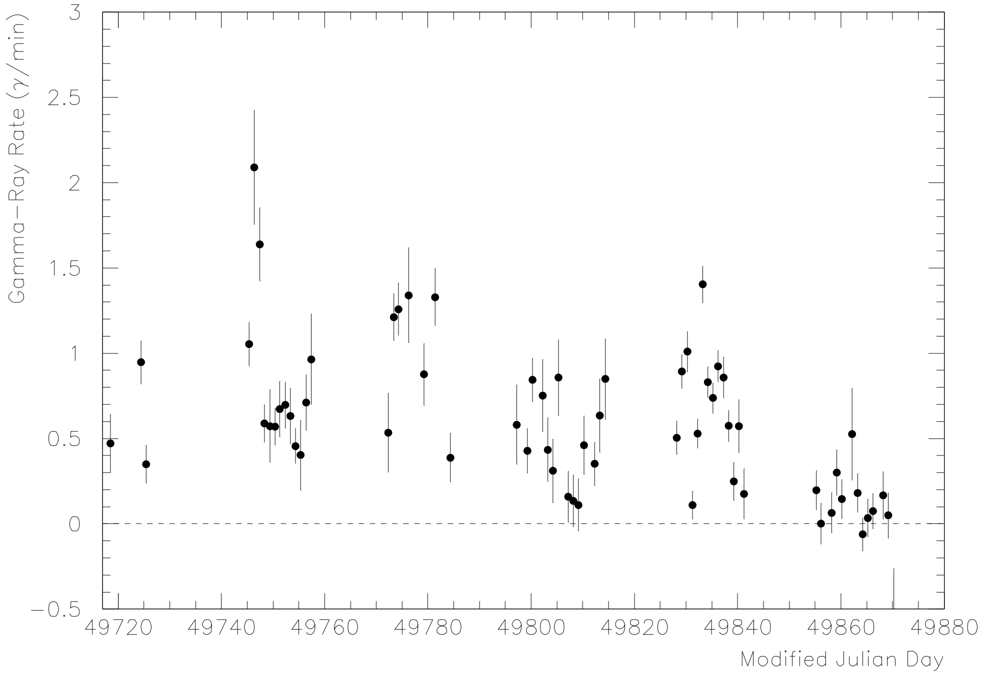

Fig. 8.— Daily VHE γ-ray count rates for Mrk 421 during 1995. Modified Julian Day 49720 corresponds to 1995 January 3. Figure from Buckley et al. (1996).

substantial amount of time observing radio-loud blazars which were not detected by EGRET. This broad approach led to the detection of the BL Lac object Mrk 501 ($z = 0.034$) by the Whipple Collaboration in 1995 (Quinn et al. 1996). A two-dimensional map of the VHE emission from Mrk 501 is shown in Figure 7. Because Mrk 501 had not been detected as a significant source of γ-rays by EGRET, this was the first object to be discovered as a γ-ray source from the ground. Hence, VHE γ-ray astronomy was established as a legitimate channel of astronomical investigations in its own right, not just an adjunct of high energy observations from space. The flux of Mrk 501 during 1995 was, on average, 10% of the VHE flux of the Crab Nebula, making it the weakest detected source of VHE γ-rays. Mrk 501 was confirmed as a source of VHE γ-rays in 1996 by the HEGRA telescopes (Bradbury et al. 1997), the CAT telescope (Punch 1997), the Telescope Array Project (Hayashida et al. 1998), and TACTIC (Bhat 1997).

In addition to the confirmed detections of Mrk 421 and Mrk 501, three other objects have recently been reported as sources of VHE γ-rays, but remain to be verified by detections from independent γ-ray telescopes. The BL Lac object 1ES 2344+514 ($z = 0.044$) was detected at energies about 350 GeV by the Whipple Observatory in 1995 (Catanese et al. 1998). Most of the emission comes from a single night, December 20, in which a flux of approximately half that of the Crab Nebula was detected with a significance of $6\,\sigma$. Other observations during that year revealed an excess of $4\,\sigma$; subsequent observations have yielded no significant signal. 1ES 2344+514 is not detected by EGRET (Thompson 1996) so if this detection is confirmed it is another instance of a γ-ray source being first detected by a ground-based telescope. PKS 2155-304 ($z = 0.117$), often considered the archetypical X-ray selected BL Lac object, was detected at energies above 300 GeV at the $7\,\sigma$ level by combining observations from 1996 and 1997 by the Durham group (Chadwick et al. 1999). The flux was approximately 40% of the VHE flux of the Crab Nebula and corresponded to an active X-ray emission period. PKS 2155-304 is an EGRET source with an average flux at $E > 100$ MeV comparable to that of Mrk 421. Finally, the BL Lac object 3C 66A ($z = 0.444$) has been reported as a source of >900 GeV γ-rays based on a $5\,\sigma$ excess seen in observations in 1996 by γ-ray telescopes at the Crimean Astrophysical Observatory (Neshpor et al. 1998). The average flux during these observations was approximately 120% of the flux of the Crab Nebula at these energies. 3C 66A is an EGRET source (Hartman et al. 1999).

Extreme variability on time-scales from minutes to years is the most distinctive feature of the VHE emission from these BL Lac objects. Variability in the emission is a surprising feature in some respects because it implies a small emission region. If low energy photons (e.g., infrared, optical, and ultraviolet) are produced in the same region, the VHE photons would pair produce with these photons and would not escape. Also, if the variability occurs near the base of the jet, there is likely to be considerable ambient radiation present which can attenuate the γ-ray signal. This opacity problem is reduced considerably if the emission is beamed toward us (e.g., Dermer & Gehrels 1995; Buckley et al. 1996), and this has been one of the main arguments for γ-ray beaming in these objects (see § 4.1.3).

The first clear detection of flaring activity in the VHE emission of an AGN came in 1994 observations of Mrk 421 by the Whipple Collaboration (Kerrick et al. 1995a) where a 10-fold increase in the flux, from an average level that year of approximately 15% of the Crab flux to approximately 150% of the Crab flux, was observed. Subsequent analysis of Mrk 421 data indicated evidence for less prominent episodes of variability during 1992 and 1993 as

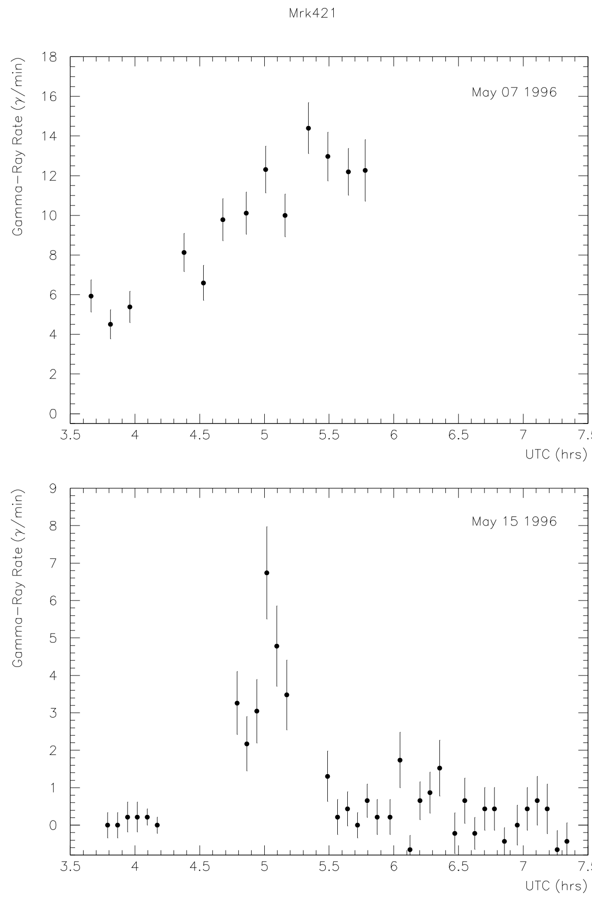

FIG. 9.— Lightcurves of two flares observed from Mrk 421 by the Whipple Collaboration on 1996 May 7 (a) and May 15 (b). The time axes are shown in coordinated universal time (UTC) in hours. For the May 7 flare, each point is a 9-minute integration; for the May 15 flare, the integration time is 4.5 minutes. Figure from Gaidos et al. (1996).

well (Schubnell et al. 1996). This suggested that variability could be present on a fairly frequent basis in the VHE emission. In order to characterize this variability, the Whipple Collaboration began systematic monitoring of Mrk 421 in 1995 which continues to the present day. The observations of Mrk 421 in 1995, shown in Figure 8, revealed several distinct episodes of flaring activity, like in previous observations, but, perhaps more importantly, indicated that the VHE emission from Mrk 421 was best characterized by a succession of day-scale or shorter flares with a baseline emission level below the sensitivity limit of the Whipple detector (Buckley et al. 1996). The time-scale of the flaring is derived from the fact that, for the most part, the flux levels measured each night varied fairly randomly with no evidence of a smooth pattern. Thus, though no significant intra-night variability was discerned in these observations, it seemed clear that it could occur.

The hypothesis that the VHE emission of Mrk 421 could flare on sub-day time-scales was borne out in spectacular fashion in 1996, with the observations of two flares by the Whipple Collaboration (Figure 9; Gaidos et al. 1996). In the first flare, observed on May 7, the flux increased monotonically during the course of $\sim$2 hours of observations, beginning at a rate twice as high as any previously observed flare and reaching a counting rate $\approx$10 times the rate from the Crab, at which point observations had to stop because of moonrise. This flux is the highest observed from any VHE source to date. The doubling time of the flare was $\sim$1 hour. Follow-up observations on May 8 showed that the flux had dropped to a flux level of $\approx$30% of the Crab Nebula flux, implying a decay time-scale of <1 day. The second flare, observed on May 15, although weaker was remarkable for its very short duration: the entire flare lasted approximately 30 minutes with a doubling and decay time of less than 15 minutes. *These two flares are the fastest time-scale variability, by far, seen from any blazar at any γ-ray energy.*

Systematic observations of Mrk 501 sensitive to day-scale flares have been conducted since 1995 with the Whipple Observatory γ-ray telescope (Quinn et al. 1999) and since 1997 with the telescopes of the HEGRA (Aharonian et al. 1999a), CAT (Punch 1997), and Telescope Array (Hayashida et al. 1998) collaborations. The results of these observations indicate a wide range of emission levels (Figure 10) and some very interesting similarities and differences with the VHE emission from Mrk 421. The observations in 1995 indicate a flux which is constant, with the exception of one night, MJD 49920, when the flux was approximately 4.6 σ above the average (approximately 5 times the flux during the remainder of the season) (Quinn

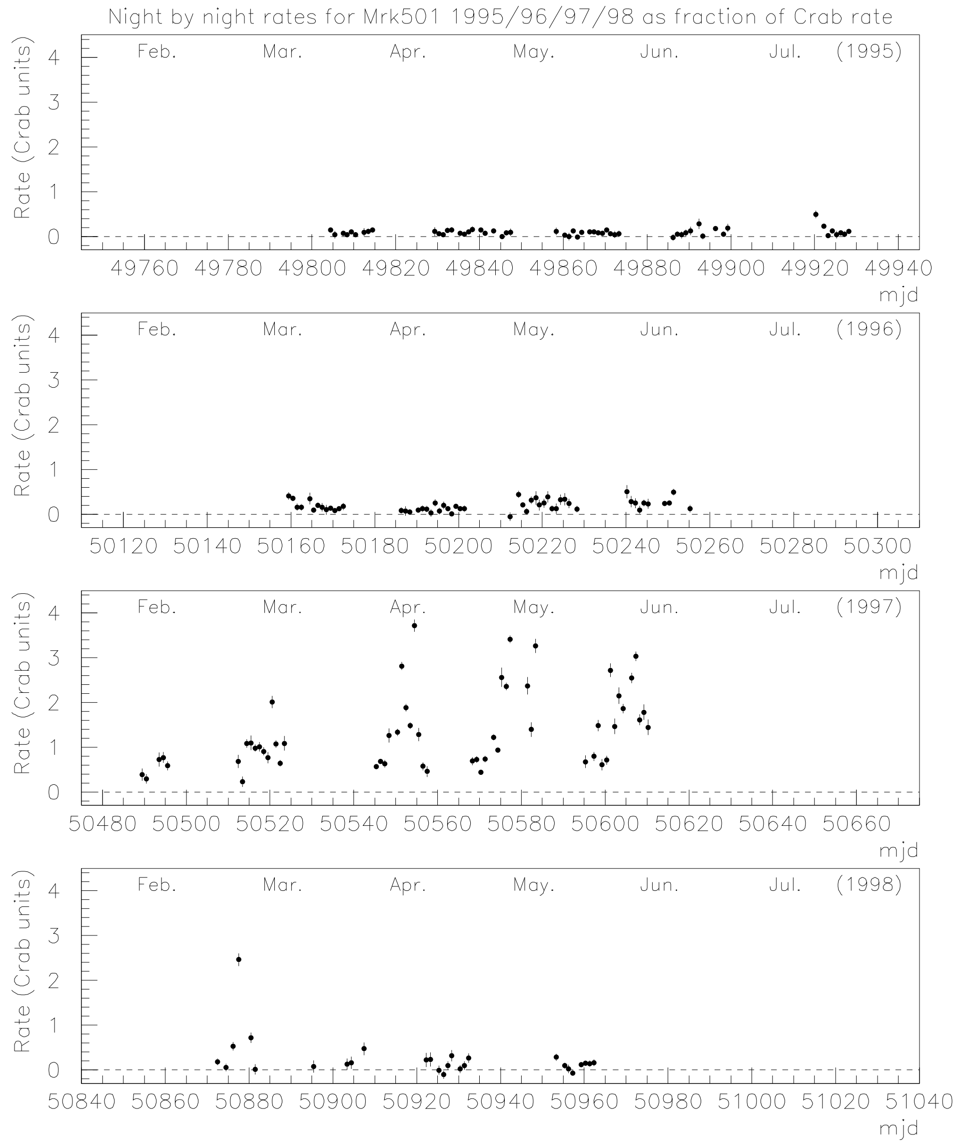

FIG. 10.— VHE γ-ray lightcurve for Mrk 501 as observed with the Whipple telescope between 1995 and 1998 at energies above 350 GeV. Fluxes are expressed as fractions of the Crab Nebula flux above 350 GeV. Figure adapted from Quinn et al. (1999).

et al. 1996; Quinn et al. 1999). Observations in 1996 by the Whipple Observatory show that the average flux of Mrk 501 had increased to approximately 20% of the Crab Nebula flux above 300 GeV indicating a two-fold increase in the average flux over the 1995 observations (Quinn et al. 1999). HEGRA observations indicated an average flux of approximately 30% of the Crab flux above 1.5 TeV, perhaps indicating a harder emission spectrum than that of the Crab Nebula. The Whipple observations show no clear flaring episodes but the probability that the average monthly flux levels are drawn from a distribution with a constant flux level is 3.6×10^{-5}, clearly indicating that the emission is varying on at least month-scales (Quinn et al. 1999). There is no significant evidence for day-scale variations within each month in 1996.

In 1997, the VHE emission from Mrk 501 changed dramatically. After being the weakest known source in the VHE sky in 1995 and 1996, it became the brightest, with an average flux greater than that of the Crab Nebula (whereas previous observations had never revealed a flux >50% of the Crab flux). Also, the amount of day-scale flaring increased and, for the first time, significant hour-scale variations were seen. Two clear episodes of hour-scale variability were detected with the Whipple Observatory telescope (Figure 11) and a search for intraday variability revealed several other nights which, considered alone, would not have been considered significant but, when combined, indicated frequent intra-day variability which was just below the sensitivity of the Whipple telescope (Quinn et al. 1999). Analysis of data from the HEGRA (Aharonian et al. 1999a) and Telescope Array (Hayashida et al. 1998) projects revealed no statistically significant intra-night variations, but the two nights in the HEGRA data with the smallest statistical probability of having constant emission are the same nights seen to have significant variability in the Whipple data.

Perhaps the most important aspect of the observations of Mrk 501 in 1997 was that, for the first time, Cherenkov

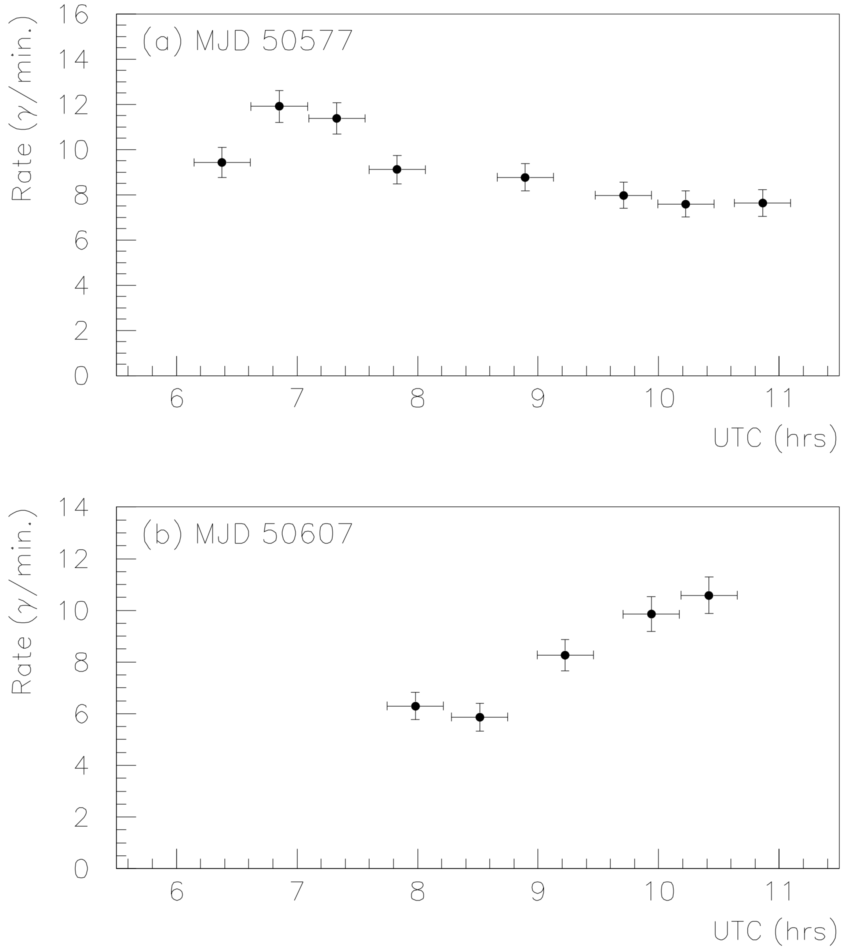

FIG. 11.— Very high energy γ-ray light curves of Mrk 501 for the two nights in 1997 which show significant intra-night variability. Figure from Quinn et al. (1999).

telescopes other than the Whipple telescope consistently detected a significant excess from Mrk 501 on a nightly time-scale. This permitted more complete VHE light-curves to be obtained (which it is expected will eventually lead to a better understanding of the VHE emission from blazars) and also provided confirmation that different VHE telescopes could obtain consistent results from a variable source (see Figure 12).

In addition to the establishment of the flaring itself, the Telescope Array Collaboration performed a periodicity search with their VHE observations of Mrk 501 in 1997 (Hayashida et al. 1998). They show evidence for a quasi-periodic signal in the data which has a period of approximately 12.7 days. This is disturbingly close to half the lunar cycle. If real this would be an extraordinary result, given the very short time-scale of the quasi-periodicity.

The only published results on observations of Mrk 501 in 1998 are those of the Whipple Observatory (Quinn et al. 1999). The average emission level was approximately 30% of the Crab flux but there was considerably more variability in the emission than in 1996 or 1995. Two distinct, very high flux flares were observed, one with the highest flux (approximately 5 times the Crab flux) ever observed from Mrk 501 with the Whipple telescope. The monthly average flux was also variable, with three months showing emission levels similar to the 1995 flux, approximately 10% of the Crab Nebula.

A natural question to ask about the variability in Mrk 501 is whether the degree of variability seen changes as a function of the mean flux level. That is, whether Mrk 501 is really more variable when its average flux is higher or whether it is an artifact of the telescopes being more sensitive to variations when the average flux is higher? To test this, Quinn et al. (1999) performed simulations to see if the day-scale variability observed with the Whipple telescope in 1997 (when the average VHE flux was 1.3 times that of the Crab) would have been detectable in 1996 and 1995 (when the average VHE flux was 20% and 10% that of the Crab, respectively) and also tested whether the month-scale variations in 1997 and 1996 would have been detectable in 1995. Their simulations indicate that the day-scale flaring in 1997 would have been detectable in the 1996 data, but not the 1995 data, and the month-scale variations in 1996 would have been detectable in 1995, while the 1997 month-scale variations would not have been detectable. Thus, it appears that the higher state emission levels have different variability characteristics than the lower emission levels.

The other unconfirmed sources are, if they are indeed sources, also variable emitters of VHE γ-rays. 1ES 2344+514 was only detected with high statistical significance on one night, but has never been detected since,

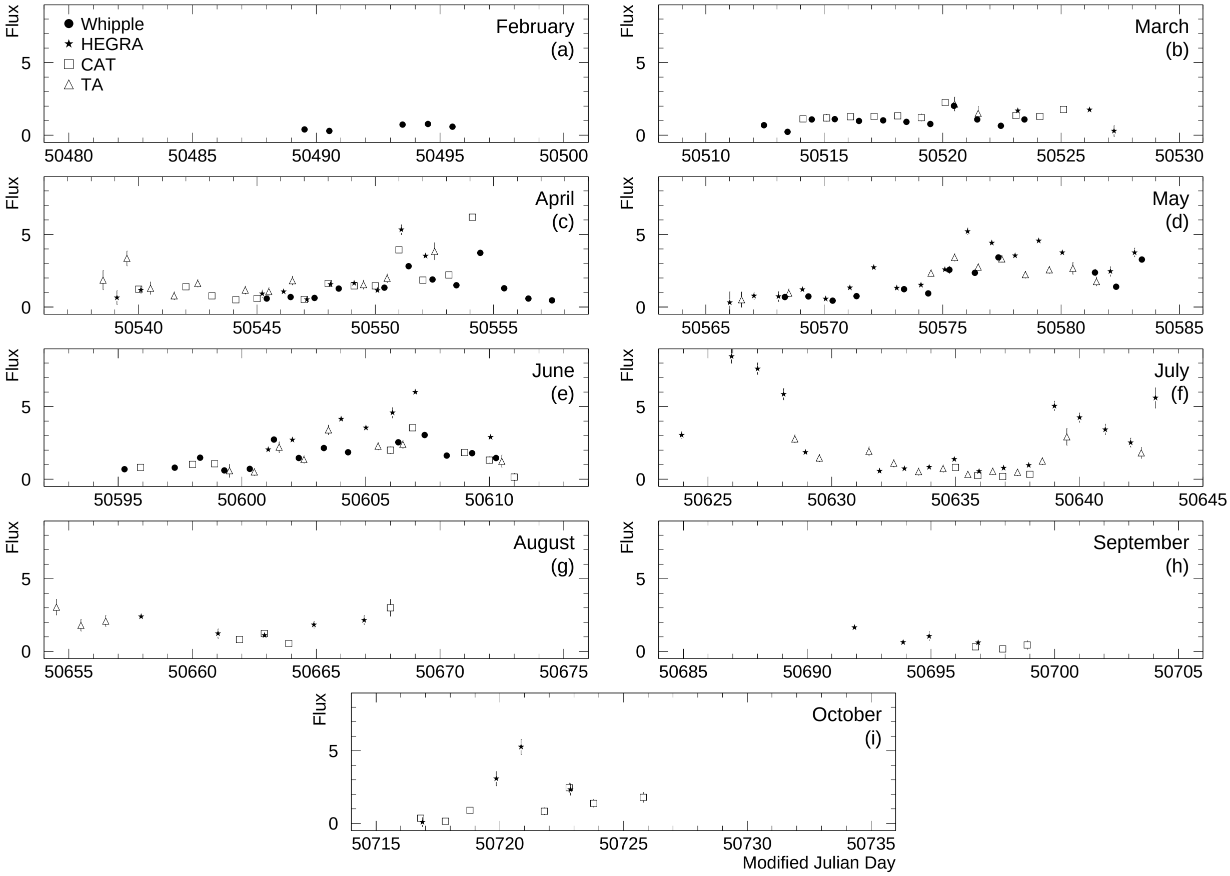

FIG. 12.— Very high energy γ-ray observations of Mrk 501 with the Whipple (filled circles, E>350 GeV), CAT (open squares, E>250 GeV), HEGRA (filled stars, E>1 TeV), and Telescope Array (open triangles, E>600 GeV) telescopes between 1997 February and October. Fluxes are shown in units of the Crab Nebula flux for the energy threshold of each telescope. The numbers on the horizontal axes for each plot indicate the Modified Julian Days during that month. Data are from Quinn et al. (1999), Aharonian et al. (1999a), Djannati-Atai et al. (1999), and Hayashida et al. (1998).

with flux limits of approximately 10% of the Crab flux (Catanese et al. 1998; Aharonian et al. 1999b). PKS 2155-304 has also been claimed to be variable (Chadwick et al. 1999), although the statistical probability that the emission is constant is not quoted. Finally, 3C 66A must be variable, or else observations with the Whipple Observatory telescope (Kerrick et al. 1995b) and the HEGRA telescope (Aharonian et al. 1999b) would have easily detected this object at the flux level quoted by the Crimean group.

The high flux VHE emission from Mrk 421 and Mrk 501 has permitted detailed spectra to be extracted. Accurate measurements of the VHE spectrum are important for a variety of reasons. First, the shape of the high energy spectrum is a key input parameter of AGN emission models, particularly as it relates to the MeV-GeV measurements by EGRET. Second, how the spectrum varies with flux, compared to longer wavelength observations provide further emission model tests. Third, spectral features, such as breaks or cut offs, can indicate changes in the primary particle distribution or absorption of the γ-rays via pair-production with low energy photons at the source or in intergalactic space (see § 4.2).

For Mrk 421, the only detailed spectra published at this time come from observations of high state emission with the Whipple Observatory telescope (Figure 13; Zweerink et al. 1997; Krennrich et al. 1999). Analysis of the spectra obtained from observations of flares on 1996 May 7 and 15 and observations of high state emission taken at large zenith angles in 1995 June indicate that, within the statistical uncertainties, the spectra are all consistent with a simple power law spectrum: $dN/dE \propto E^{-2.5}$ (Krennrich et al. 1999). When combined, these three data sets are consistent with a simple power law spectrum for Mrk 421 of the form (Krennrich et al. 1999)

$$\frac{dN}{dE}\ (250\,\mathrm{GeV} - 10\,\mathrm{TeV})\ \propto E^{-2.54 \pm 0.03_{\mathrm{stat}} \pm 0.10_{\mathrm{syst}}}$$

where E is in TeV.

Observations of Mrk 421 in 1997 and 1998 with the HEGRA system of Cherenkov telescopes reveal a significantly different spectrum (Aharonian et al. 1999c)

$$\frac{dN}{dE}\ (500\,\mathrm{GeV} - 7\,\mathrm{TeV})\ \propto E^{-3.09 \pm 0.07_{\mathrm{stat}} \pm 0.10_{\mathrm{syst}}}$$

than observed with the Whipple telescope. The emission level for the HEGRA observations was approximately 0.5 times the Crab flux, much lower than the fluxes (1 – 10 times the Crab flux) used in the Whipple observations. This may indicate that the spectrum in Mrk 421 becomes softer with decreasing flux. However, HEGRA observations show no evidence of variability between observations at fluxes above the Crab flux and those between one-sixth

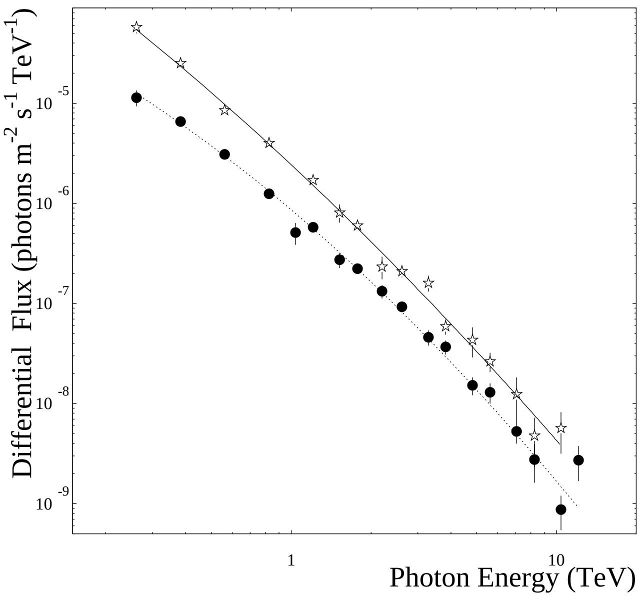

FIG. 13.— VHE γ-ray spectra of Mrk 421 (open stars) and Mrk 501 (filled circles) as measured with the Whipple Observatory telescope (from Krennrich et al. 1999). The solid line through the Mrk 421 points indicates the best-fit spectrum to these data and the dashed line through the Mrk 501 points is the best-fit spectrum for those data.

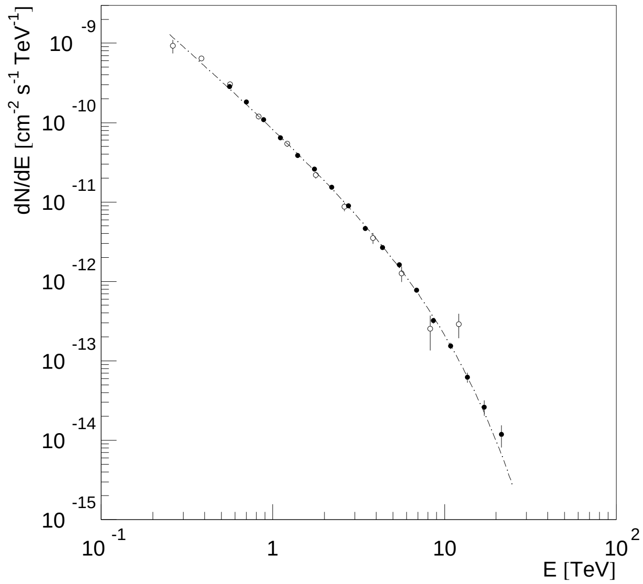

FIG. 14.— The energy spectrum of Mrk 501 as measured by the HEGRA array (filled circles) and the Whipple telescope (open circles). The dashed line indicates the power law plus exponential cut-off spectrum fit to the HEGRA data. Figure from Konopelko (1999).

and one-half the Crab flux and the Whipple results show no variations in spectral index despite using observations spanning a 10-fold range of fluxes. Further studies may help resolve these differences.

As with the studies of the variability of its VHE flux, the high state emission detected from Mrk 501 in 1997 allowed detailed spectra to be derived by several experiments, permitting studies of the time-dependence of the spectra and providing all-important cross-checks of the methods used to derive energy spectra. Because of the rapid variability of the emission, again the normalization of the spectra are not of fundamental importance, except perhaps in the context of multi-wavelength studies which are discussed in § 4.1.2 below.

The most detailed energy spectra published at this time come from Whipple observations between 250 GeV and 12 TeV (Samuelson et al. 1998; Krennrich et al. 1999) and HEGRA data spanning 500 GeV to 20 TeV (Aharonian et al. 1999b). The Telescope Array Collaboration has also derived a spectrum over a slightly narrower energy range (600 GeV to 6.5 TeV) (Hayashida et al. 1998). A search for variability in the spectrum revealed no significant changes in spectrum with flux or time (Samuelson 1999; Aharonian et al. 1999a), allowing large data sets to be combined to derive very detailed energy spectra spanning large ranges in energy. The spectra derived by Whipple and HEGRA deviate significantly from a simple power law. For Whipple, the χ^2 probability that a power law is consistent with the measured spectrum is 2.5×10^{-7}. This is the first significant deviation from a power law seen in any VHE γ-ray source and any blazar at energies above 10 MeV. The Whipple spectrum is:

$$\frac{\mathrm{dN}}{\mathrm{dE}} \propto \mathrm{E}^{-2.22\pm0.04_{\mathrm{stat}}\pm0.05_{\mathrm{syst}}-(0.47\pm0.07_{\mathrm{stat}} log_{10}(E))}$$

and the HEGRA spectrum is:

$$\frac{\mathrm{dN}}{\mathrm{dE}} \propto \mathrm{E}^{-1.92\pm0.03_{\mathrm{stat}}\pm0.20_{\mathrm{syst}}} * \exp\left[-\frac{\mathrm{E}}{6.2\pm0.4_{\mathrm{stat}}(-1.5+2.9)_{\mathrm{syst}}}\right]$$

where E is in units of TeV. The form of the curvature term in the spectra has no physical significance as the energy resolution of the experiments is not sufficient to resolve particular spectral models. The Whipple spectral form is simply a polynomial expansion in logE v. log(dN/dE) space. The HEGRA form was chosen presumably because attenuation of the VHE γ-rays by pair-production with background IR photons could produce an exponential cut-off. In fact, the Whipple and HEGRA data are completely consistent with each other as shown in Figure 14. The Telescope Array Collaboration derived a spectrum which is well fit by a simple power law (dN/dE $\propto E^{-2.5\pm0.1}$). The data from this spectrum are also consistent with the Whipple and HEGRA spectra.

4.1.2. *Multi-wavelength observations*

Some of the most exciting results on VHE γ-ray sources have come through observations where several telescopes operating at different wavelengths simultaneously monitor the activity in a blazar. These multi-wavelength campaigns have involved the larger astronomical community in the study of VHE sources and served the subsidiary purpose of confirming the source identifications of the VHE γ-ray emitting blazars.

The first evidence of correlated variability between VHE γ-rays and lower energy emission came from a multi-wavelength campaign on Mrk 421 in 1994 April/May (Macomb et al. 1995, Macomb et al. 1996). Observations were conducted with the Whipple telescope, EGRET, the *Advanced Satellite for Cosmology and Astrophysics* (*ASCA*)

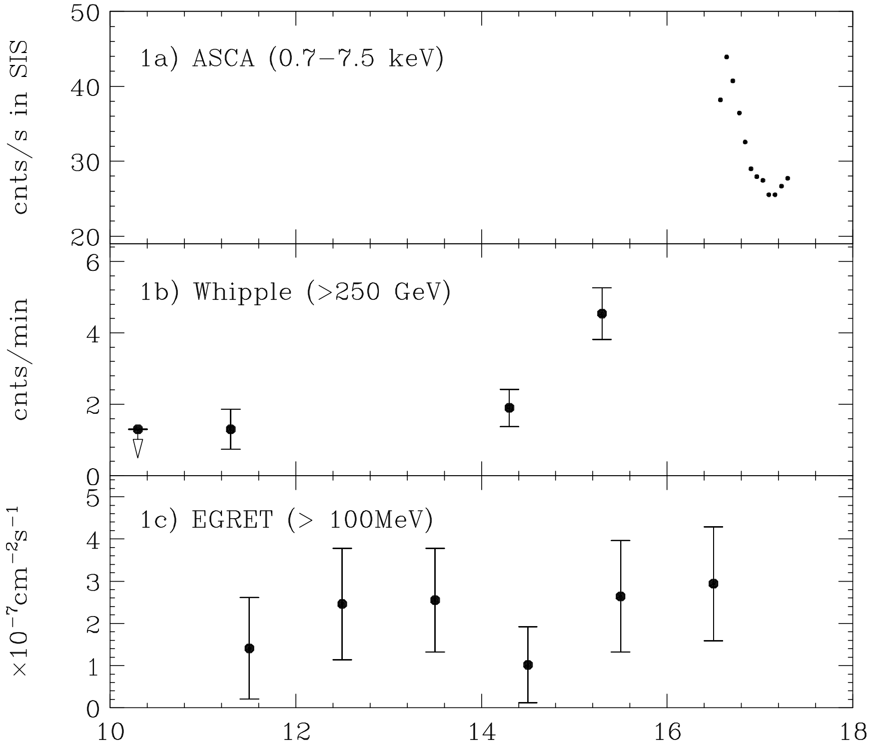

FIG. 15.— Lightcurves for observations of Mkn 421 in 1994 May by *ASCA* (top), Whipple (middle), and EGRET (bottom). Figure from Takahashi, Madejski, and Kubo (1999).

in X rays, the International Ultraviolet Explorer (IUE), the United Kingdom Infrared Telescope (UKIRT), the James Clerk Maxwell Telescope (JCMT) in the mm waveband, and the University of Michigan 26-m radio telescope (UMRAO) in the 4.8 – 14.5 GHz frequency range. The VHE γ-ray, *ASCA*, and EGRET observations are shown in Figure 15. The VHE observations reveal the rising edge of a flare that developed over approximately 4 days with the peak flux detected on May 15 (UT) being approximately 9 times the mean flux measured during that observing season and approximately 1.4 times the flux of the Crab Nebula. Observations had to be halted after May 15 because the phase of the moon precluded further observations. Observations taken with *ASCA* on May 16/17 (Takahashi et al. 1994, 1996) indicated a flux approximately 20 times the quiescent X-ray flux of Mrk 421, and the time coincidence between the two observations of unprecedented high states is the basis for the claim of a correlation in this campaign. Interestingly, EGRET observations taken between 1997 May 10 and 17 did not detect the strong day-scale variability seen in VHE γ-rays. The average flux during this period was approximately twice the average flux measured in 1994 April, so there is some evidence of a higher emission state, but it is not significant enough to claim a correlation. The observations at UV, IR, mm, and radio wavelengths showed no evidence of variability during this period. Because of the offset in time of the observations between the VHE γ-rays and the X rays, detailed comparisons of the variability in those wavebands are not possible.

Spurred by this result, another multiwavelength campaign was organized in 1995 to better measure the multiwavelength properties of Mrk 421. This campaign revealed, for the first time, correlations between VHE γ-rays and X rays (Buckley et al. 1996). Observations were conducted between April 20 and May 5 with the Whipple telescope, EGRET, *ASCA*, the *Extreme Ultraviolet Explorer* (*EUVE*), an optical telescope, an optical polarimeter, and UMRAO. Observations with EGRET did not result in a detection of Mrk 421. The 2σ flux upper limit for E>100 MeV is 1.2×10^{-7} cm^{-2} s^{-1}, somewhat below the level detected in 1994. The light curves for some of these observations are shown in Figure 16. The optical data have the contribution from the host galaxy of Mrk 421 subtracted off. As in the 1994 multiwavelength campaign, Mrk 421 underwent a large amplitude flare in VHE γ-rays during the observations. The flare is also clearly seen in the *ASCA* and *EUVE* observations. There is some evidence for correlated variability in the optical flux and polarization, but the statistics are not good enough to be confident about claiming such an association. The X rays and VHE γ-rays appear to vary together, limited to the one day resolution of the VHE observations, and the amplitude of the flaring is similar, $\sim$400% difference between the peak flux and that at the end of the observations. The EUVE and optical data (assuming it also is correlated) are consistent with the flare being delayed by approximately 1 day relative to the X rays and VHE γ-rays. The amplitude of the flare also decreases with decreasing energy. The XUV flux varies by $\sim$200% during the observations and the optical flux varies by about 20%. The B-band percent polarization varies by nearly a factor of two in the observations.

The observations of Mrk 421 in 1994 and 1995 were clearly undersampled, limiting the conclusions that could be drawn concerning correlations between wavelengths and emission models. Two multiwavelength campaigns organized in 1998 attempted to improve these measurements

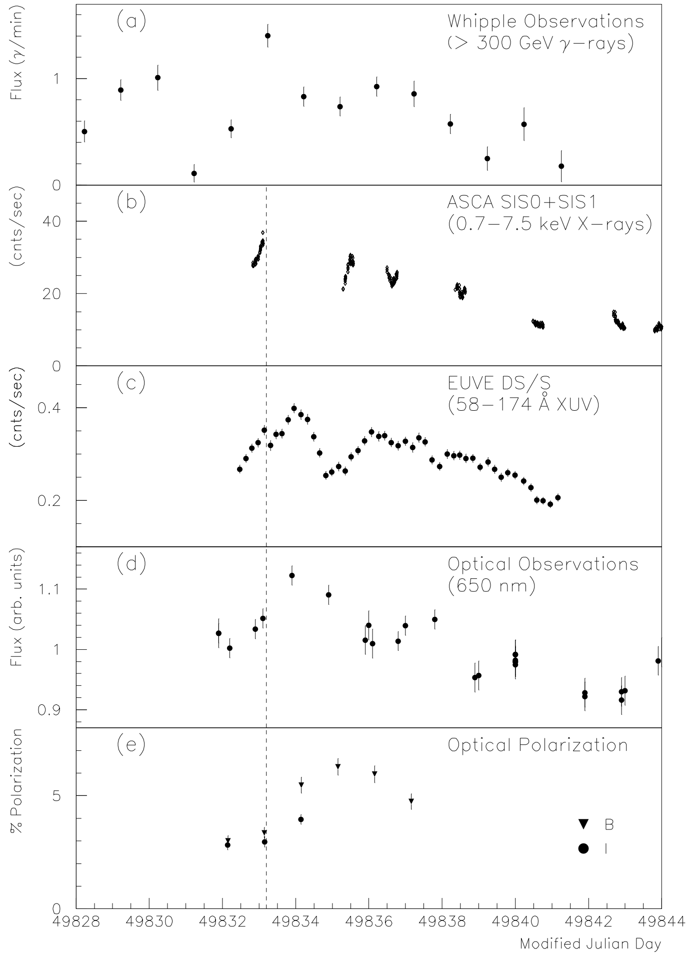

FIG. 16.— (a) Gamma-ray, (b) X-ray, (c) extreme-UV, (d) optical, and (e) optical polarization measurements of Mrk 421 taken 1995 April – May. April 26 corresponds to MJD 49833. Figure from Buckley et al. (1996).

through more dense observations in X rays and VHE γ-rays. Improvement in the VHE measurements came about through longer VHE exposures with individual telescopes, to search for hour-scale variations, and coordination of VHE observations between CAT, HEGRA, and Whipple. Thus, light curves of 12 – 16 hours could in principle be achieved, allowing much more detailed measurements of the VHE emission. These observations yielded immediate improvements in the measurements of flaring activity and correlations between VHE γ-rays and X rays.

The first campaign, conducted in late 1998 April, was centered at X-ray wavelengths on observations with the *BeppoSAX* satellite and established the first hour-scale correlations between X rays and γ-rays in a blazar (Maraschi et al. 1999). The lightcurve for the observations by *BeppoSAX* in three X-ray bands and Whipple above 2 TeV is shown in Figure 17. The VHE threshold here is higher than typical of Whipple data because observations were taken at a wide range of elevations, causing the energy threshold and sensitivity to vary with time. These effects were corrected in the light curve through the use of simulations and analysis cuts to normalize the collection area and energy threshold. Thus, the VHE lightcurve rate variations are intrinsic. As Figure 17 shows, a flare is clearly detected in X rays and TeV γ-rays on the first day of observations. The peaks in the lightcurves occur at the same time, within 1 hour, but the fall off in the X-ray flux is considerably slower than the TeV γ-rays. Also, the TeV γ-rays have a larger variability amplitude ($\sim$4-fold ratio between average and peak) than the X rays ($\sim$2-fold). Both the faster VHE flux decrease and the larger amplitude variability have not been seen previously in Mrk 421. These observations provide the first clear indication that X rays and VHE γ-rays may not be completely correlated on all time-scales.

The second multiwavelength campaign started in late 1998 April, immediately after the observations discussed above, and was centered around a seven day continuous observation of Mrk 421 with *ASCA* (Takahashi et al. 1999). The light curves for the X-ray observations and VHE observations by Whipple, CAT, and HEGRA are shown in Figure 18. Had these observations been conducted as in 1994 and 1995, with short X-ray exposures and just Whipple observations, the results would have shown nothing new: similar variability scale between the X rays and VHE γ-rays and some sub-dayscale X-ray variability with amplitude too low to be resolved with the Whipple observations. Instead, the X-ray observations reveal the complete cycle of about 10 flares, the first time this has been done for Mrk 421. Also, these observations seem to confirm the supposition of Buckley et al. (1996) that the VHE emission from Mrk 421 is primarily the result of flares, with

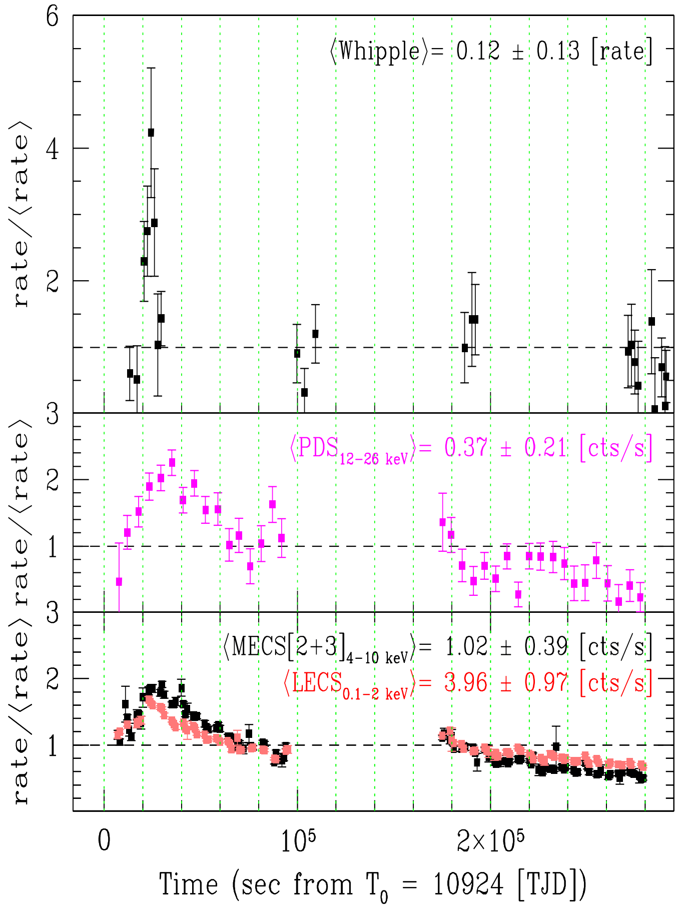

Fig. 17.— Lightcurves for observations of Mrk 421 in 1998 April by Whipple and *BeppoSAX*. Whipple observations are for E>2 TeV and are binned in 28-minute observing segments. All count rates are normalized to their respective averages (listed at the top of each panel) for the observations shown. Figure from Maraschi et al. (1999).

little steady emission evident. Finally, the combination of VHE data from these telescopes confirms the sub-day-scale correlations seen in the Whipple/*BeppoSAX* observations. Detailed comparisons of the VHE γ-ray and X-ray data will require more sophisticated normalization of the VHE data (e.g., to common threshold energies) and investigation of systematics in the measures of variability, but the data hold the promise of significantly advancing our study of VHE-emitting γ-ray blazars. They also clearly demonstrate the benefits of operating multiple VHE γ-ray installations in understanding the nature of variable sources.

The first multi-wavelength observations of Mrk 501 which included VHE observations were conducted in 1996 (Kataoka et al. 1999). The observations were conducted with the Whipple telescope, EGRET, *ASCA*, and an optical telescope. The light curve for these observations is shown in Figure 19. The observations were too undersampled, or insensitive in the case of EGRET, to clearly establish any correlations, but these observations have two very important results. First, follow up observations in 1996 May established the first detection of Mrk 501 by EGRET, with a marginal significance of 4.0σ above 100 MeV but a significance of 5.2σ above 500 MeV indicating a hard photon spectrum (Kataoka et al. 1999). The claim of a $3.5\,\sigma$ detection by EGRET during a small part of the multiwavelength campaign (the region between the dashed lines in Figure 19) seems speculative, given the lack of any increased activity in other wavebands during that period. Second, the observations established a baseline spectral energy distribution for Mrk 501 during a relatively low emission state which could be compared to observations of the high state emission in 1997 (see below for discussion of spectral energy distributions).

Multiwavelength observations of Mrk 501 during its high emission state in 1997 revealed, for the first time, clear correlations between its VHE γ-ray and X-ray emission (Catanese et al. 1997). Observations were conducted with Whipple (nightly, from April 7-19), EGRET and Oriented Scintillation Spectrometer Experiment (OSSE) on *CGRO* (April 9 – 15), *BeppoSAX* (April 7, 11, 16), *RXTE* (twice nightly April 3 – 16), and the Whipple Observatory 1.2-m optical telescope (nightly, April 7 – 15). The optical and X-ray observations were serendipitously scheduled at this time, and the *CGRO* observations were a public target of opportunity observation initiated in response to the high VHE emission state.

Figure 20 shows daily flux levels for the contemporaneous observations of Mrk 501. The average flux level in the U-band in March is also included in the figure (Fig. 20e, *dashed line*) to indicate the significant ($\gtrsim$10%) increase in

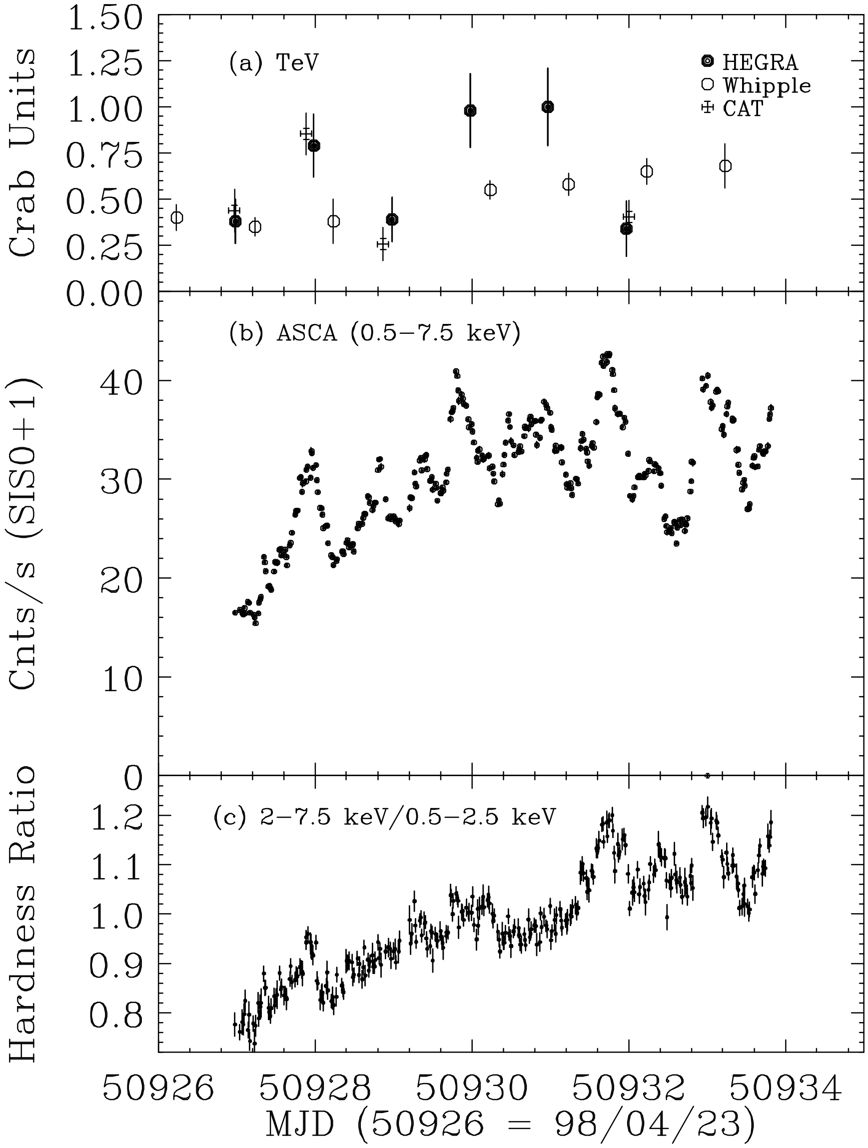

Fig. 18.— Lightcurves for observations of Mrk 421 in 1998 April – May. (a) VHE flux observed with HEGRA, Whipple, and CAT, (b) X-ray flux observed with *ASCA*, and (c) X-ray hardness ratios observed with *ASCA* are shown. Figure from Takahashi et al. (1999).

flux between March and April. An 11 day rise and fall in flux is evident in the VHE and X-ray wavebands, with peaks on April 13 and 16. The 50 – 150 keV flux detected by OSSE also increases between April 9 and 15, with a peak on April 13. The optical data may show a correlated rise, but the variation is small (at most 6%). Subtraction of the galaxy light contribution will increase the amplitude of this variation, but it should still remain lower than in X rays, given that the R-band contribution of the galaxy light is ∼75% (Wurtz, Stocke & Yee 1996) and the U-band contribution should be much less. EGRET observations indicated an excess of 1.5σ, not a significant detection. The ratio of the fluxes between April 13 and April 9 are 4.2, 2.6, 2.3, and 2.1 for the VHE γ-ray, OSSE, *RXTE*, 15 – 25 keV, and *RXTE* 2 – 10 keV emission, respectively.

The results of this campaign show that for Mrk 501, like Mrk 421, the VHE γ-rays and the soft X rays vary together and the variability in the synchrotron emission increases with increasing energy. However, OSSE has never detected Mrk 421 despite several observations (McNaron-Brown et al. 1995), while the Mrk 501 detection had the highest 50 – 150 keV flux ever detected by OSSE from a blazar. A likely explanation of the OSSE detection is that the synchrotron emission in Mrk 501 extends to 100 keV, compared with the ∼1 keV cutoff seen in Mrk 421. This explanation was first confirmed by the observations with *BeppoSAX* (Pian et al. 1998). In addition, the day scale variations for Mrk 501 are larger in γ-rays than in X rays, unlike Mrk 421. So, despite the similarity of Mrk 421 and Mrk 501 in some respects, these multi-wavelength campaigns are beginning to reveal differences in the two objects.

In these short multi-wavelength campaigns, there appears to be a correlation between the X rays and VHE γ-rays. A natural question to ask is whether this is always true, or only during certain situations. An attempt to answer this question has been made by the HEGRA collaboration by comparing their observations of Mrk 501 above 500 GeV to those by the *RXTE* All-Sky Monitor, measuring 2 – 12 keV photons (Aharonian et al. 1999a). A cross-correlation analysis of the daily average flux mea-

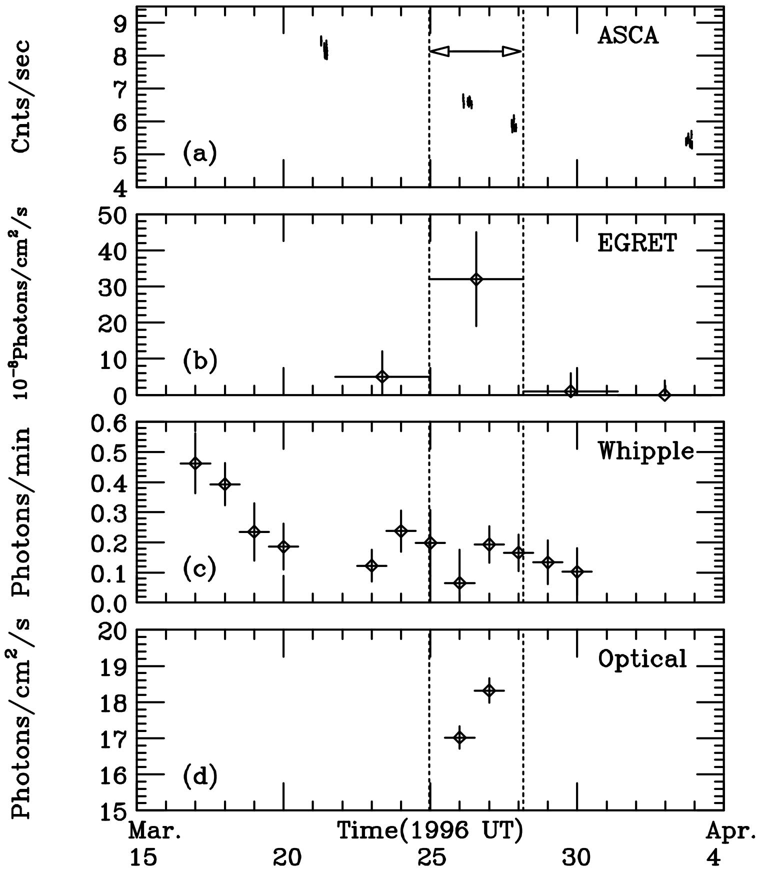

FIG. 19.— Lightcurve for observations of Mrk 501 in 1996 March. Observations in (a) 0.7 – 10 keV X rays (*ASCA*), (b) 100 MeV – 10 GeV γ-rays (EGRET), (c) >350 GeV γ-rays (Whipple), and (d) R-band, 650 nm, optical are shown. Figure from Kataoka et al. (1999).

sured by the All-Sky Monitor with the daily average flux measured by HEGRA reveals a peak in the correlation function at $\Delta t = 0 \pm 1$ day. However, the peak in the cross-correlation function is only ~0.4 and the significance of the peak is only 2σ – 3σ. Whether this indicates that the X-ray/TeV correlation is *not* present is unclear because the ASM data have large statistical and significant systematic uncertainties for day-scale measurements of this relatively dim X-ray source (i.e., compared to the X-ray binaries the ASM was designed to monitor). Also, because HEGRA sits on the falling edge of the high energy spectrum and the ASM sits (for Mrk 501 in 1997) on the rising edge of the synchrotron spectrum, it is possible that the emission detected by these two instruments will not be completely correlated, particularly for day-scale variations. Comparison of longer-term variability between the measurements might help resolve such issues.

Figure 21 shows the spectral energy distributions (SEDs), expressed as power per logarithmic bandwidth, for Mrk 421 and Mrk 501 derived from contemporaneous multi-wavelength observations and an average of non-contemporaneous archival measurements. Both have a peak in the synchrotron emission at X-ray frequencies, as is typical of X-ray selected BL Lac objects, and a high energy peak whose exact location is unknown but must lie in the $10 - 250$ GeV range. Both the synchrotron and high energy peak are similar in power output, unlike the EGRET-detected flat-spectrum radio quasars which can have high energy peaks well above the synchrotron peaks (e.g., von Montigny et al. 1995). Also, during flaring episodes, the X-ray spectrum in both objects tends to harden significantly (Takahashi et al. 1996, 1999; Pian et al. 1998) while the VHE spectrum is not observed to change.

The SEDs of the two sources do, however, exhibit important differences. Most prominent among these is that the combination of contemporaneous *RXTE* and OSSE observations of Mrk 501 in 1997 clearly confirm the initial measurements of Pian et al. (1998) that the synchrotron spectrum extended well-beyond the ~1 keV typical of X-ray selected BL Lac objects. They also establish that the peak power output of the synchrotron emission occurs at ~100 keV. This is in contrast to the 1996 observations of Mrk 501 reported by Kataoka et al. (1999), where the synchrotron power peak is at ~2 keV. For Mrk 421, the X-ray spectral peak does shift to higher energies during flaring activity, but the changes are much smaller than in Mrk 501, and the peak was never observed to extend beyond ~1 keV. This peak is followed by a sharp cutoff which produces a deficit in the OSSE range, preventing the detection of Mrk 421 by this instrument.

Whether the shift in the location of the synchrotron peak for Mrk 501 is also accompanied by a shift in the onset of the γ-ray emission to higher energies is not clear. Any increase in the MeV-GeV flux in 1997 was not as great as at TeV energies, or EGRET would have easily detected Mrk 501. But, because the sensitivity of EGRET in 1997 was substantially poorer than in 1996, a shift in the onset of the spectrum or a flux variation that increases

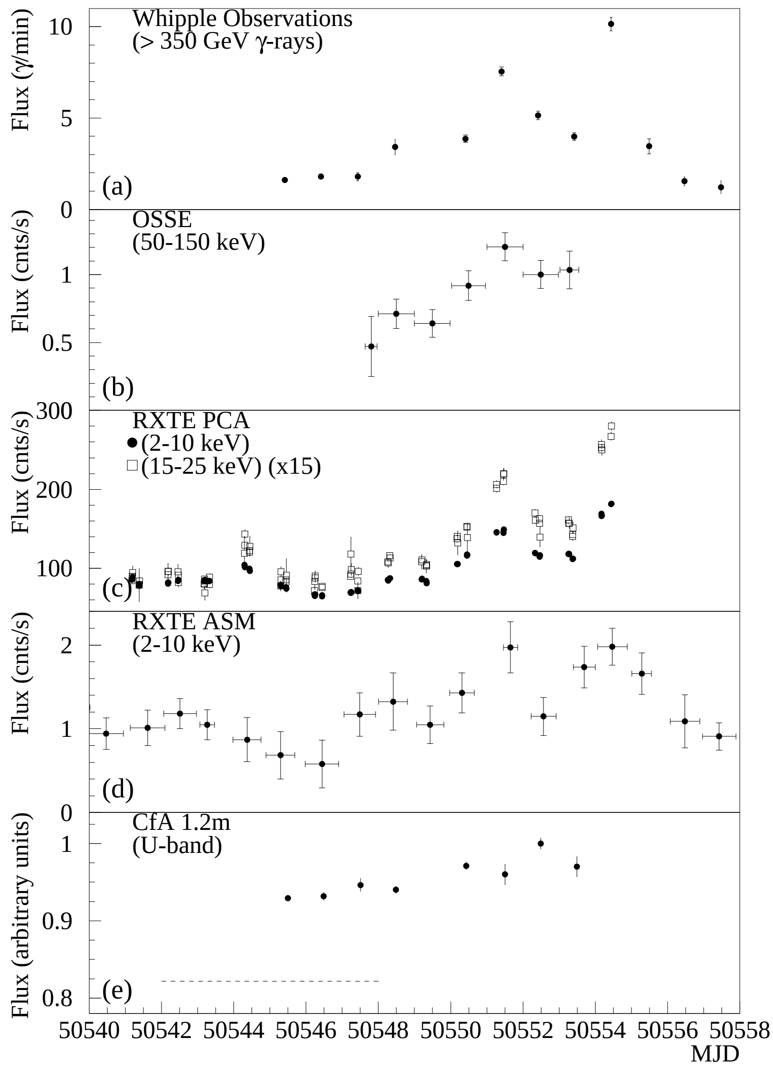

Fig. 20.— (a) VHE γ-ray, (b) OSSE 50 – 150 keV, (c) *RXTE* 2 – 10 keV and 15 – 25 keV, (d) *RXTE* All-Sky Monitor 2 – 10 keV, and (e) U-band optical light curves of Mrk 501 for the period 1997 April 2 (MJD 50540) to April 20 (MJD 50558). The dashed line in (e) indicates the average U-band flux in 1997 March. Whipple, OSSE, ASM, and optical data are from Catanese et al. (1997) and *RXTE* data are from Catanese (1999).

with increasing energy could explain the non-detection by EGRET. The fact that the VHE spectrum of Mrk 501 is harder than that of Mrk 421 below $\sim$1 TeV (see Figure 13) may also indicate that the high energy peak of Mrk 501 is shifted to slightly higher energies. However, it could also simply indicate a slower fall off in the progenitor particle spectrum above the peak power output.

A second difference in the spectral energy distributions for these two objects is that the power output for Mrk 501 in the VHE range can be considerably less than in X rays when it is in a low emission state. In contrast, Mrk 421 seems to maintain a similar output at X-ray and γ-ray energies. These differences are illustrated in Table 5 which gives the ratio of contemporaneously measured fluxes for X rays and γ-rays for these two objects. Whether the difference in power output for Mrk 501 reflects a change of the energy at which the peak in the high energy spectrum occurs or something related to the flaring process is not clear, due to the poor spectral measurements in the low emission states and the lack of coverage of the peak region of the spectrum. However, the lack of spectral variability in γ-rays argues against a significant short-term shift of the γ-ray spectral peak.

4.1.3. *Implications of the Very High Energy Observations*

The general properties of the detected extragalactic sources of VHE γ-rays are listed in Table 6. The three objects detected by the Whipple Collaboration exhibit some interesting commonalities. They are the three closest known BL Lac objects with declination $> 0°$ so their γ-ray fluxes are the least attenuated from interaction with background IR radiation. The >100 MeV fluxes are near (Mrk 421, Mrk 501) or below (1ES 2344+514) the EGRET sensitivity limit, meaning that the γ-ray power output does not peak in that energy range as it does for many of the EGRET-detected AGNs (von Montigny et al. 1995). Thus, VHE observations already augment the catalog of γ-ray sources compiled by space-borne telescopes. Finally, all three of the Whipple-detected BL Lac objects are X-ray selected BL Lac objects (XBLs). The extension of the synchrotron spectra to X-ray energies in XBLs implies that they produce high energy electrons, making

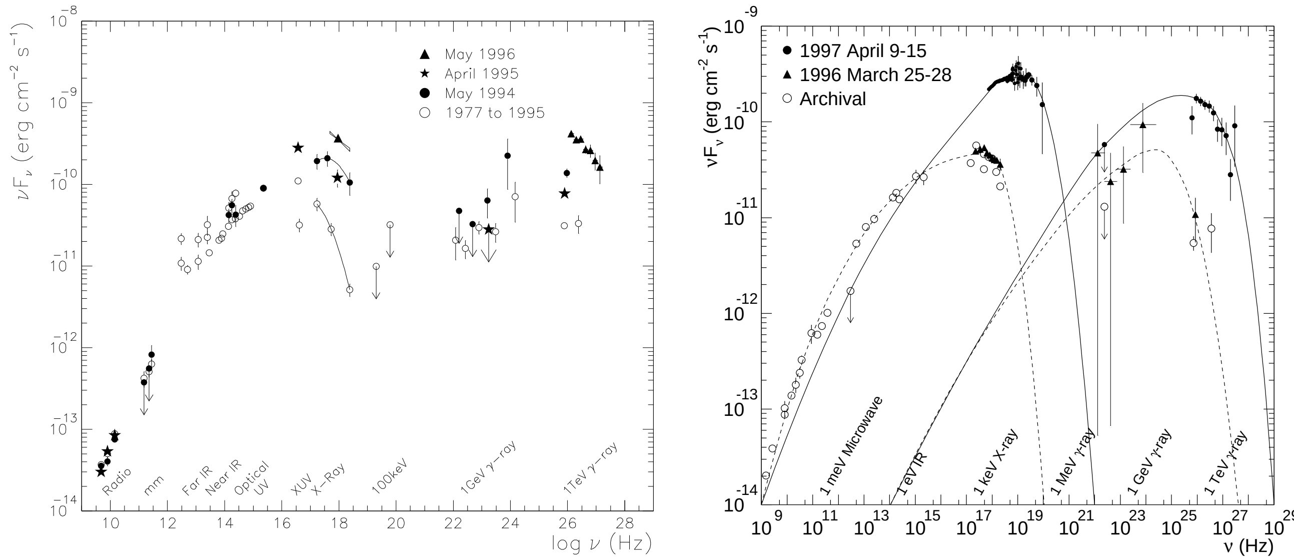

Fig. 21.— Left: The spectral energy distribution of Mrk 421 from contemporaneous and archival observations. Dates of the observations are indicated in the figure. Figure from Buckley et al. (1997). Right: The spectral energy distribution of Mrk 501 from contemporaneous and archival observations. Dates of the observations are indicated in the figure. Data in the figure come from Kataoka et al. (1999), Catanese et al. (1997), and Catanese (1999) and references therein. The curves in the figure are meant to guide the eye to the contemporaneously measured points, and do not indicate model fits to the data nor are they an attempt to elucidate the spectral energy distribution of Mrk 501 during these observations. In both figures, the archival measurements are approximate averages of the data in the literature.

Table 5

Spectral energy ratios for VHE sources

Source	Date	$R^a_{2\,\mathrm{keV}}$	$R^b_{100\,\mathrm{keV}}$	$R^c_{100\,\mathrm{MeV}}$	Ref.
Mrk 421	1995	2.2±0.5		<0.38	Buckley et al. 1996
	1996	0.81±0.06			Buckley et al. 1997
Mrk 501	1996	4.4±2.1		3.1±3.4	Kataoka et al. 1999
	1997	1.2±0.3	1.9±0.5	<0.36	Catanese et al. 1997; Catanese 1999

[a] $\nu F_\nu(2\,\mathrm{keV})/\nu F_\nu(350\,\mathrm{GeV})$

[b] $\nu F_\nu(100\,\mathrm{keV})/\nu F_\nu(350\,\mathrm{GeV})$

[c] $\nu F_\nu(100\,\mathrm{MeV})/\nu F_\nu(350\,\mathrm{GeV})$

them good candidates for VHE emission if the VHE γ-rays are produced via inverse Compton (IC) scattering of these same electrons. EGRET's tendency to detect more radio-selected BL Lac objects (RBLs) than XBLs (Lin et al. 1997) also supports this tenet because RBLs would be expected to have spectra which peak in the MeV-GeV range (Sikora et al. 1994; Marscher & Travis 1996). BL Lac objects in general have been suggested as better candidates for VHE emission than other blazars because the absence of optical emission lines in BL Lac objects may indicate less VHE-absorbing radiation near the emission region (Dermer & Schlickeiser 1994).

The other two objects detected at VHE energies, PKS 2155-304 and 3C 66A, are similar in some respects to the Whipple sources. PKS 2155-304 is an XBL, so it fits the IC paradigm for VHE sources. However, 3C 66A is classified as an RBL, suggesting that protons produce the γ-rays because in IC models, RBLs would not have high enough energy electrons to produce TeV emission. In addition, both PKS 2155-304 and 3C 66A are at much higher redshifts than the Whipple sources, implying quite low IR backgrounds. Thus, confirmation of these detections, just as for 1ES 2344+514, is essential.

VHE observations have already significantly affected our understanding of BL Lac objects. For example, the rapid variability indicates either very low accretion rates and photon densities near the nucleus (Celotti, Fabian & Rees 1998) or, conversely, requires the γ-ray emission region to be located relatively far from the nucleus to escape the photon fields (Protheroe & Biermann 1997). Also, the observations have helped resolve the nature of the differences between RBLs and XBLs. Based on their smaller numbers and higher luminosities, Maraschi et al. (1986) proposed that RBLs were the same as XBLs but with jets aligned more closely with our line of sight. However, the rapid variability and TeV extent of the XBL emission point to the differences between the two sub-classes being more fundamental, as originally proposed by Padovani & Giommi (1994): the XBLs have higher maximum electron energies and lower intrinsic luminosities.

Simultaneous measurements of the synchrotron and VHE γ-ray spectra also constrain the magnetic field strength (B) and Doppler factor (δ) of the jet. If the correlation between the VHE γ-rays and optical/UV pho-

Table 6
Properties of the VHE BL Lac objects

Object	z	EGRET flux[a] (E>100 MeV) (10^{-7}cm^{-2}s^{-1})	Average flux (E>300 GeV) (10^{-12}cm^{-2}s^{-1})	M_v [a]	$\mathcal{F}_X$ [a] (2 keV) (μJy)	$\mathcal{F}_R$ [a] (5 GHz) (mJy)
Mrk 421	0.031	1.4±0.2	40	14.4	3.9	720
Mrk 501	0.034	3.2±1.3	≥8.1	14.4	3.7	1370
1ES 2344+514[c]	0.044	<0.7	$\lesssim$8.2	15.5	1.1	220
PKS 2155-304[c]	0.116	3.2±0.8	42	13.5	5.7	310
3C 66A[c]	0.444	2.0±0.3	30[b]	15.5	0.6	806

[a]Radio, optical, and X-ray data from Perlman et al. (1996). EGRET data from D.J. Thompson (priv. comm.), Mukherjee et al. (1997), and Kataoka et al. (1999).
[b] >1 TeV flux value.
[c] Unconfirmed as a VHE source.

tons observed in 1995 from Mrk 421 indicates both sets of photons are produced in the same region of the jet, $\delta \gtrsim 5$ is required for the VHE photons to escape significant pair-production losses (Buckley et al. 1996). If the SSC mechanism produces the VHE γ-rays, $\delta = 15 - 40$ and $B = 0.03 - 0.9$G for Mrk 421 (Buckley et al. 1997; Tavecchio, Maraschi & Ghisellini 1998; Catanese 1999) and $\delta \approx 1.5 - 20$ and $B = 0.08 - 0.2$G for Mrk 501 (Samuelson et al. 1998; Tavecchio et al. 1998; Hillas 1999). To match the variability time-scales of the correlated emission, proton models which utilize synchrotron cooling as the primary means for proton energy losses require magnetic fields of $B = 30 - 90$G for $\delta \approx 10$ (Mannheim 1993; Mannheim 1998; Buckley 1998). The Mrk 421 values of δ and B are extreme for blazars, but they are still within allowable ranges and are consistent with the extreme variability of Mrk 421.

In addition, the VHE observations have constrained the types of models that are likely to produce the γ-ray emission. For instance, the correlation of the X-ray and the VHE flares is consistent with IC models where the same population of electrons radiate the X rays and γ-rays. The absence of flaring at EGRET energies may also follow in this context (Macomb et al. 1995) because the lower energy electrons which produce the γ-rays in the EGRET range radiate away their energy more slowly than the higher energy electrons which produce the VHE emission. The MeV-GeV emission could then be the superposition of many flare events and would therefore show little or no short-term variation.

In the mechanism of Sikora et al. (1994), which produces γ-rays through the Comptonization of external photons, the external photons must have energies < 0.1 eV (in the IR band) to avoid significant attenuation of the VHE γ-rays by pair production. Sikora et al. (1994) point out that there is little direct observational evidence of such an IR component in BL Lac objects, but the existence of such a field has been predicted as a product of accretion in AGNs (Rees et al. 1982).

Models which produce the γ-ray emission from proton progenitors through e^+e^- cascades originating close to the base of the AGN jet have great difficulty explaining the TeV emission observed in Mrk 421 because the high densities of unbeamed photons near the nucleus, such as the accretion disk or the broad line region, required to initiate the cascades cause high pair opacities to TeV γ-rays (Coppi, Kartje & Königl 1993). Such models also predict that the radius at which the optical depth for γ-γ pair production drops below unity increases with increasing γ-ray energy (Blandford & Levinson 1995) and therefore the VHE γ-rays should vary either later or more slowly than the MeV-GeV γ-rays. This is in contradiction to the observations of Mrk 421 in both 1994 (Macomb et al. 1995) and 1995 (Buckley et al. 1996).

4.2. *Extragalactic Background Light*

In traversing intergalactic distances, γ-rays may be absorbed by photon-photon pair production ($\gamma + \gamma \rightarrow e^+ + e^-$) on background photon fields if the center of mass energy of the photon-photon system exceeds twice the rest energy of the electron (Gould & Schréder 1967). The cross-section for this process peaks when

$$\mathrm{E}_\gamma \epsilon (1 - \cos\theta) \sim 2(m_e c^2)^2 = 0.52(\mathrm{MeV})^2 \quad (1)$$

where E_γ is the energy of the γ-ray, ϵ is the energy of the low energy photon, θ is the collision angle between the two photons, m_e is the mass of the electron, and c is the speed of light in vacuum. Thus, for photons of energy near 1 TeV, head-on collisions with photons of $\sim$0.5 eV have the highest cross-section, though a broad range of optical-to-IR wavelengths can be important absorbers because the cross-section for pair production is rather broad in energy and spectral features in the extragalactic background density can make certain wavebands more important than the cross-section alone would indicate.

The presence of extragalactic background light (EBL) limits the distance to which VHE γ-ray telescopes can detect sources. This has been put forth as an explanation of the lack of detection of many of the EGRET-detected AGNs (e.g., Stecker, de Jager & Salamon 1992), as discussed above. The difficulty in understanding the effect of the EBL on the opacity of the universe to VHE γ-rays is that not much is known about the spectrum of the EBL at present, nor how it developed over time. Star formation is expected to be a major contributor to the EBL (e.g., Madau et al. 1996; Primack et al. 1999), with star formation contributing mainly at short wavelengths (1 – 15 μm) and dust absorption and re-emission contributing at longer wavelengths (15 – 50 μm) . So, measurements of the EBL spectrum can serve as important tracers of the history of the formation of stars and galaxies (Dwek et al. 1998). Other, more exotic processes, such as pre-galactic star formation and some dark matter candidates, might also contribute distinctive features to the EBL (e.g., Bond, Carr & Hogan 1986, 1991). Thus, measurements of the EBL have the potential to provide a wealth of information about several important topics in astrophysics.

Experiments that attempt to measure the EBL by directly detecting optical-IR photons, such as the Diffuse Infrared Background Experiment (DIRBE) on the *Cosmic Background Explorer* (*COBE*), are plagued by foreground sources of IR radiation. Emitted and scattered light from interplanetary dust, emission from unresolved stellar components in the Galaxy, and dust emission from the interstellar medium are all significantly more intense than the EBL and must be carefully modelled and subtracted to derive estimates of the EBL. Currently, EBL detections are available only at 140 μm and 240 μm (Hauser et al. 1998). Tentative detections at 3.5 μm (Dwek & Arendt 1998) and 400 – 1000 μm (Puget et al. 1996) have also been reported.

Because VHE γ-rays are attenuated most by optical-IR photons, measurements of the spectra of AGNs provide an indirect means of investigating the EBL that is not affected by local sources of IR radiation (Gould & Schréder 1967; Stecker, de Jager & Salamon 1992). The signs of EBL absorption can be cutoffs, but also simple alterations of the spectral index (e.g., Stecker 1999), depending on the spectral shape of the EBL and the distance to the source. Like direct measurements of the EBL, this technique has difficulties to overcome. For instance, it requires some knowledge of or assumptions about the intrinsic spectrum and flux normalization of the AGNs or the EBL. Also, the AGNs themselves produce dense radiation fields which can absorb VHE γ-rays at the source and thereby mimic the effects of the intergalactic EBL attenuation.

Despite these difficulties, the accurate measurement of VHE spectra with no obvious spectral cut-offs from just the two confirmed VHE-emitting AGNs, Mrk 421 and Mrk 501 (see § 4.1.1), has permitted stringent limits to be set on the density of the EBL over a wide range of wavelengths. These limits have been derived from two approaches: (1) assuming a limit to the hardness of the intrinsic spectrum of the AGNs and deriving limits which assume very little about the EBL spectrum (e.g., Biller et al. 1998; Stanev & Franceschini 1998) and (2) assuming some shape for the EBL spectrum, based on theoretical or phenomenological modelling of the EBL, and adjusting the normalization of the EBL density to match the measured VHE spectra (e.g., de Jager, Stecker & Salamon 1994; Stanev & Franceschini 1998). The latter can be more stringent, but are necessarily more model-dependent. The limits from these indirect methods and from the direct measurements of EBL photons are summarized in Figure 22. At some wavelengths, the TeV limits represent a 50-fold improvement over the limits from DIRBE. These limits are currently well above the predicted density for the EBL from normal galaxy formation (Madau et al. 1996; Primack et al. 1999), but they have provided constraints on a variety of more exotic mechanisms for sources of the EBL (e.g., Biller et al. 1998). They also show that EBL attenuation alone cannot explain the lack of detection of EGRET sources with nearby redshifts at VHE energies, as the optical depth for pair-production does not reach 1 for the stringent limits of Biller et al. (1998) until beyond a redshift of $z = 0.1$ (see Figure 23). With the detection or more AGNs, particularly at higher redshift, and improvements in our understanding of the emission and absorption processes in AGNs, VHE measurements have the potential to set very restrictive limits on the EBL density, and perhaps eventually detect it.

4.3. *Gamma-Ray Bursts*

Although the γ-ray burst phenomenon is usually associated with energies of 100 keV to 1 MeV (hard X rays to low energy γ-rays) results from EGRET show that there is a component at high energies and thus the phenomenon has the potential to be observed in the TeV range. The power spectrum certainly peaks in the lower energy ranges but the observations at high energies really provide the strongest constraints on the emission models and may ultimately expose the underlying emission mechanism. The detection of a single photon of energy 18 GeV from GRB 970217, 1.5 hours after the onset of the burst (Hurley et al. 1994), has opened the possibility of delayed emission of GeV-TeV photons (e.g., Totani 1998; Bottcher & Dermer 1998). Although ACITs have, to date, only presented upper limits (e.g., Connaughton et al. 1997), it is possible that in the near future wide field air shower detectors like MILAGRO or the Tibet Array might detect a prompt VHE emission component and rapid slew ACITs might do the same with greater sensitivity for any delayed emission.

5. THE FUTURE OF VHE ASTRONOMY

It is clear that to fully exploit the potential of ground-based γ-ray astronomy the detection techniques must be improved. This will happen by extending the energy coverage of the technique (with good energy resolution) and by increasing its flux sensitivity (improved angular resolution and increased background rejection). Ideally one would like to do both but in practice there must be trade-offs. Reduced energy threshold can be achieved by the use of larger, but cruder, mirrors and this approach is currently being exploited using existing arrays of solar heliostats: STACEE (Chantell et al. 1998), CELESTE (Quebert et al. 1995) and Solar-2 (Tümer et al. 1999). A German-Spanish project (MAGIC) (Barrio et al. 1998) to build a 17-m aperture telescope has also been approved. These projects will achieve thresholds as low as 20-30 GeV where they will effectively fill the current gap in the γ-ray spectrum from 20 to 200 GeV. Ultimately, this gap will be covered by GLAST (Gehrels & Michelson 1999). Extension to higher energies (>10 TeV) can be achieved by atmospheric Cherenkov telescopes working at large zenith angles and by particle arrays on very high mountains. An interesting telescope that has just come on line and will complement these techniques is the MILAGRO water Cherenkov detector in New Mexico which will operate 24 hours a day with a large field of view and will have good sensitivity to γ-ray bursts and transients (Sinnis et al. 1995).

VERITAS, with seven 10-m telescopes arranged in a hexagonal pattern with 80 m spacing (Figure 24), will aim

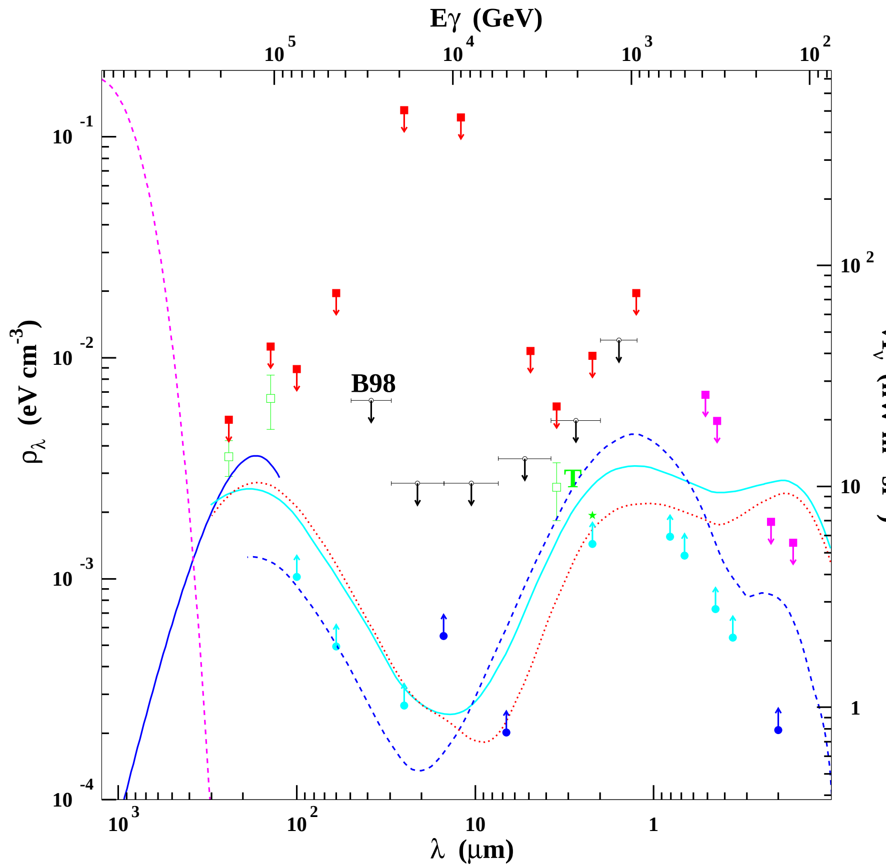

FIG. 22.— The diffuse intergalactic infrared background. E_γ is the energy at which the pair-production cross-section peaks for head on collisions with photons of wavelength λ. Upper limits derived from VHE γ-ray spectra are indicated by the horizontal bars with arrows, marked as B98 (Biller et al. 1998). Filled squares are upper limits from various experiments measuring the EBL directly (Hauser et al. 1998; Bowyer 1991; Maucherat-Joubert, Deharveng & Cruvellier 1980; Toller 1983; Dube, Wickes & Wilkinson 1979). The open squares at 140 μm and 240 μm are detections from DIRBE (Hauser et al. 1998). The open square marked "T" indicates a tentative detection (Dwek & Arendt 1998). The filled circles are lower limits derived from galaxy counts (Hacking & Soifer 1991; Oliver et al. 1997; Stanev & Franceschini 1998; Pozzetti, Bruzual & Zamorani 1996; Pozzetti et al. 1998; Armand, Milliard & Deharveng 1994). The solid curve between 90 μm and 150 μm is a FIRAS detection (Fixsen et al. 1994). The dashed line on the left indicates the 2.7 K cosmic microwave background radiation. The three curves spanning most of the IR wavelengths are different models of Primack et al. (1999). Figure courtesy of V. Vassiliev.

for the middle ground between those techniques listed above, with its primary objective being high sensitivity observations in the 100 GeV to 10 TeV range (Weekes et al. 1999). It will be located in southern Arizona and will be a logical progression from the Whipple telescope. It is hoped to begin construction in 1999 and to complete the array by 2004.

The German-French-Italian experiment HESS, initially four and eventually perhaps sixteen 12m class telescopes in Namibia (Hofmann 1997), and the Japanese Super CANGAROO array, with four 10-m telescopes in Australia, (T. Kifune, private communication) will have similar objectives. In each case, the arrays will exploit the high sensitivity of ACITs and the high selectivity of the array approach. The projected sensitivities of MAGIC, HESS, SuperCANGAROO and VERITAS are somewhat similar and we refer to them collectively as Next Generation Gamma-Ray Telescopes (NGGRTs). The relative flux sensitivities for existing and planned γ-ray telescopes as a function of energy are shown in Figure 25, where the sensitivities of the wide field detectors are for one year and the atmospheric Cherenkov telescopes are for 50 hours. In all cases, a 5 σ point source detection is required.

It is apparent from this figure that, on the low energy side (<1 TeV), the NGGRTs will complement the GLAST mission and will overlap with the solar arrays. At the highest energies to which they are sensitive, NGGRTs will overlap with the Tibet Air Shower Array (Amenomori et al. 1997). They will cover the same energy range as MILAGRO but with greater flux sensitivity. The wide field coverage of MILAGRO will permit the detection of transient sources which, once detected, can be studied in more detail by the northern NGGRTs. These same telescopes will complement the coverage of neutrino sources to be discovered by AMANDA/ICE CUBE (Halzen 1998) at the South Pole. Finally, if the sources of ultra-high energy cosmic rays are localized to a few degrees by HiRes (Abu-Zayyad et al. 1997) and Auger (Boratav 1997), the NGGRTs will be powerful instruments for their further localization and identification.

The recent successes in VHE γ-ray astronomy ensure that in the inevitable interval between the death of EGRET and the launch of the next generation γ-ray space telescope, there will be ongoing activity in GeV-TeV γ-ray astronomy. Observations by GLAST and the NGGRTs in this energy region will make important contributions to our understanding of AGNs, supernova remnants, and pulsar and γ-ray burst studies. Although the number of

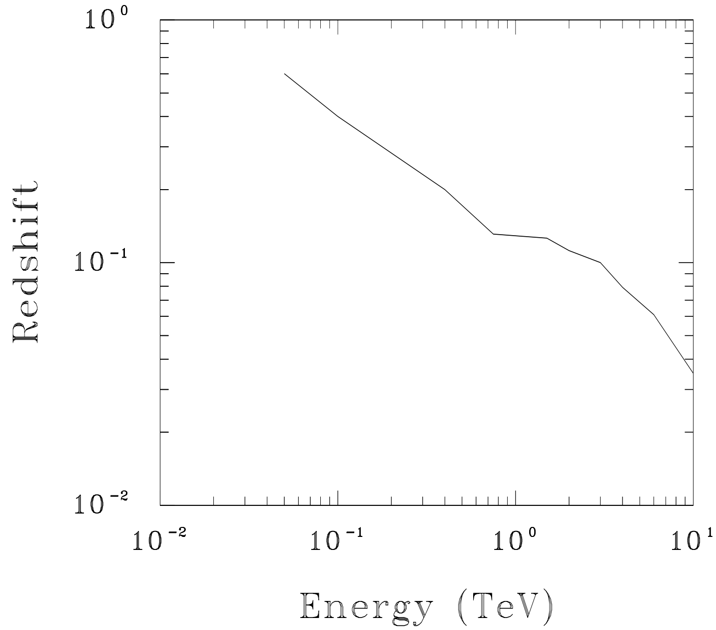

FIG. 23.— Lower limit of the redshift at which photons of the energies shown face an optical depth of 1 due to pair-production with EBa.L Limits are derived from the upper limits on the density of the EBL of Biller et al. (1998). Figure from Biller et al. (1998).

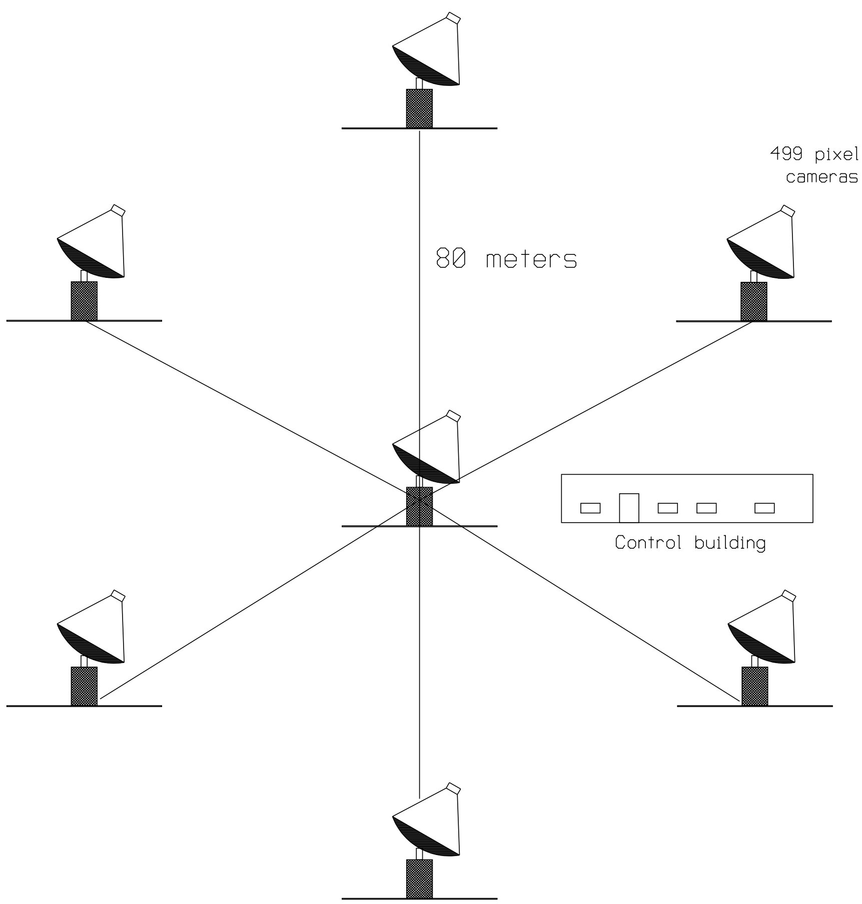

FIG. 24.— The proposed arrangement of telescopes in VERITAS. Figure from Weekes et al. (1999).

TeV sources detected so far is small, the new and varied phenomena observed indicate that VHE γ-ray astronomy is not merely an extension of MeV-GeV γ-ray astronomy but is a discipline in its own right. With the advent of new telescopes, the catalog of VHE γ-ray sources will dramatically expand with detailed time histories and accurate

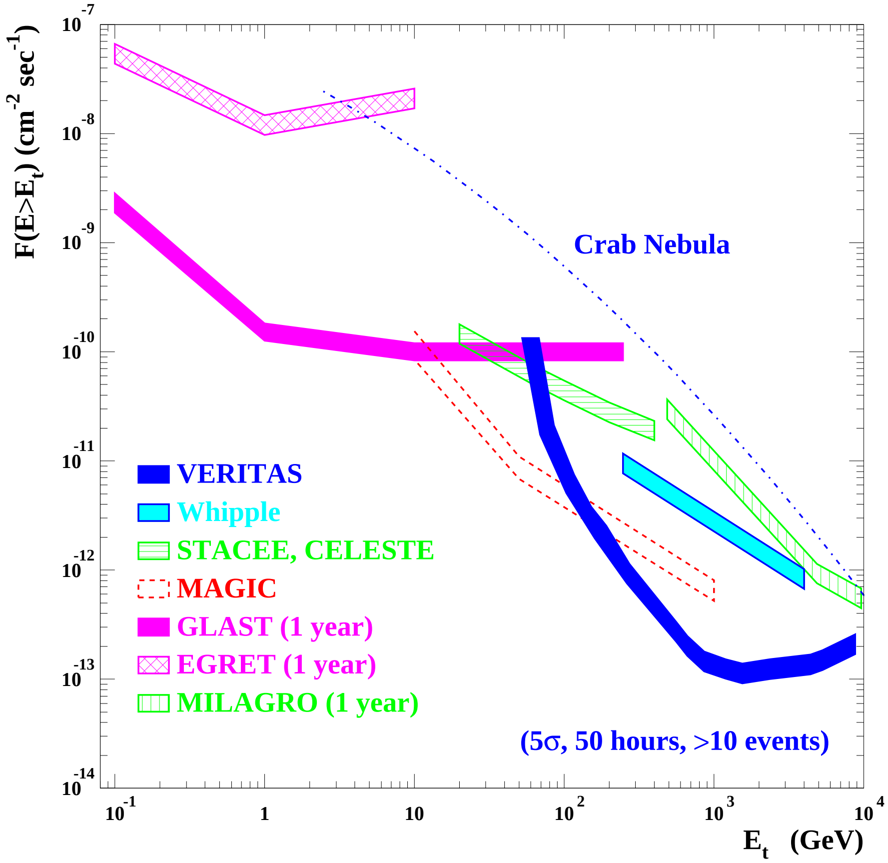

FIG. 25.— Comparison of the point source sensitivity of VERITAS to Whipple (Weekes et al. 1989), MAGIC (Barrio et al. 1998), CELESTE/STACEE (Quebert et al. 1995; Chantell et al. 1998); HEGRA (Daum et al. 1997), GLAST (Gehrels & Michelson 1999), EGRET (Thompson et al. 1993), and MILAGRO (Sinnis et al. 1995). The sensitivity of MAGIC is based on the availability of new technologies, e.g., hybrid PMTs, not assumed in the other experiments. EGRET, GLAST and MILAGRO are wide field instruments and therefore ideally suited for all sky surveys. The turn-up in the VERITAS sensitivity at higher energies is primarily caused by the requirement that the signal contain at least 10 photons.

energy spectra available.

We thank F. Aharonian, A. Djannati-Atai, F. Kajino, J. Kataoka, M. Punch, T. Takahashi, D. Thompson, and V. Vassiliev for providing some of the data and figures presented here, and A. Burdett and S. Fegan for reading the manuscript. This research is supported by grants from the U. S. Department of Energy and NASA.

REFERENCES

Abu-Zayyad, T., et al. 1997, in Proc. 25th Internat. Cosmic Ray Conf. (Durban, South Africa), ed. M. S. Potgeier, B. C. Raubenheimer, & D. J. van der Walt, 5, 325
Aharonian, F.A., & Akerlof, C.A. 1997, Ann. Rev. Nucl. Part. Sci., 47, 273
Aharonian, F. A., et al. 1999a, A&A, 342, 69
Aharonian, F. A., et al. 1999b, A&A, submitted (astro-ph/9903455)
Aharonian, F. A., et al. 1999c, A&A, submitted (astro-ph/9905032)
Aiso, S., et al. 1997, in Proc. 25th Internat. Cosmic Ray Conf. (Durban, South Africa), ed. M. S. Potgeier, B. C. Raubenheimer, & D. J. van der Walt, 3, 261
Akerlof, C. W., et al. 1993, A&A, 274, L17
Allen, G. E., et al. 1995, ApJ, 448, L25
Amenomori, M. et al. 1997, in Proc. 25th Internat. Cosmic Ray Conf. (Durban, South Africa), ed. M. S. Potgeier, B. C. Raubenheimer, & D. J. van der Walt, 5, 245
Armand, C., Milliard, B., Deharveng, J. M. 1994, A&A, 284, 12
Barrau, A., et al. 1998, Nucl. Instrum. Methods A, 416, 278
Barrio, J.A., et al. 1998, "The Magic Telescope", design study, MPI-PhE/98-5
Bell, A. R. 1978, MNRAS, 182, 147
Bhat, C. L. 1997, IAUC, 6709
Biller, S. D., et al. 1998, Phys. Rev. Lett., 80, 2992
Blandford, R. D., & Levinson, A. 1995, ApJ, 441, 79
Blandford, R. D., & Ostriker, J. P. 1978, ApJ, 221, L29
Blandford, R. D., & Rees, M. J. 1978, in Pittsburgh Conf. on BL Lac Objects, ed. A. M. Wolfe (Pittsburgh: Univ. Pittsburgh Press), 328
Bloom, S. D., & Marscher, A. P. 1996, ApJ, 461, 657
Bond, J. R., Carr, B. J., & Hogan, C. J. 1986, ApJ, 306, 428
Bond, J. R., Carr, B. J., & Hogan, C. J. 1991, ApJ, 367, 420
Boratav, M. 1997, in Proc. 25th Internat. Cosmic Ray Conf. (Durban, South Africa), ed. M. S. Potgeier, B. C. Raubenheimer, & D. J. van der Walt, 5, 205
Borione, A., et al. 1995, in Proc. 24th Internat. Cosmic Ray Conf. (Rome), 2, 439
Bottcher, M., & Dermer, C. D. 1998, ApJ, 499, L131
Bowyer, S. 1991, ARA&A, 29, 59
Bradbury, S. M., et al. 1997, A&A, 320, L5
Brazier, K. T. S., Kanbach, G., Carraminana, A., Guichard, J., & Merck, M. 1996, MNRAS, 281, 1033
Buckley, J. H. 1998, Science, 279, 676
Buckley, J. H., et al. 1996, ApJ, 472, L9
Buckley, J. H., et al. 1997, in Proc. of the Fourth Compton Symp., ed. C. D. Dermer, M. S. Strickman, & J. D. Kurfess (New York: AIP), AIP Conf. Proc. 410, 1381
Buckley, J. H., et al. 1998, A&A, 329, 639
Catanese, M. 1999, in BL Lacertae Phenomenon, ed. L. O. Takalo & A. Silanpaa (San Francisco: ASP), ASP Conf. Series, 159, 243
Catanese, M., et al. 1997, ApJ, 487, L143
Catanese, M., et al. 1998, ApJ, 501, 616

Cawley, M. F., et al. 1985, in Proc. 19th Internat. Cosmic Ray Conf. (La Jolla, Calif.), ed. F. C. Jones, J. Adams, & G. M. Mason (Washington, D.C.: NASA), NASA Conf. Publ. 2376, 1, 264
Celotti, A., Fabian, A. C., & Rees, M. J. 1998, MNRAS, 293, 239
Chadwick, P. M., et al. 1997, in Proc. 25th Internat. Cosmic Ray Conf. (Durban, South Africa), ed. M. S. Potgeier, B. C. Raubenheimer, & D. J. van der Walt, 3, 189
Chadwick, P. M., et al. 1999, ApJ, 513, 163
Chantell, M.C., et al. 1998, Nucl. Instrum. Methods A, 408, 468
Connaughton, V., et al. 1997, ApJ, 479, 859
Coppi, P. S., Kartje, J. F., & Königl, A. 1993, in Proc. of the Compton Symposium, ed. M. Friedlander, N. Gehrels, & D. J. Macomb (New York: AIP), 559
Daugherty, J. K., & Harding, A. K. 1982, ApJ, 252, 337
Daum, A., et al. 1997, Astropart. Phys., 8, 1
Dermer, C. D., & Gehrels, N. 1995, ApJ, 447, 103
Dermer, C. D., & Schlickeiser, R. 1994, ApJS, 90, 945
Dermer, C. D., Schlickeiser, R., & Mastichiadis, A. 1992, A&A, 256, L27
Djannati-Atai, A., et al. 1999, A&A, submitted
Drury, L. O'C., Aharonian, F. A., & Völk, H. J. 1994, A&A, 287, 959
Drury, L. O'C., Markiewicz, W. J., & Völk, H. J. 1989, A&A, 225, 179
Dube, R. R., Wickes, W. C., Wilkinson, D. T. 1979, ApJ, 232, 333
Dwek, E., & Arendt, R. G. 1998, ApJ, 508, L9
Dwek, E., et al. 1998, ApJ, 508, 106
Esposito, J. A., et al. 1996, ApJ, 461, 820
Fixsen, D. J., Dwek, E., Mather, J. C., Bennett, C. L., & Shafer, R. A. 1994, ApJ, 508, 123
Fossati, G., Maraschi, L., Celotti, A., Comastri, A., & Ghisellini, G. 1998, MNRAS, 299, 433
Gaidos, J. A., et al. 1996, Nature, 383, 319
Gaisser, T. K., Protheroe, R. J., & Stanev, T. 1998, ApJ, 492, 219
Gehrels, N., & Michelson, P. 1999, in TeV Astrophysics of Extragalactic Sources, ed. M. Catanese & T. C. Weekes, Astropart. Phys., in press
Georganopoulos, M., & Marscher, A. P. 1998, ApJ, 506, 621
Ghisellini, G., Celotti, A., Fossati, G., Maraschi, L., & Comastri, A. 1998, MNRAS, 301, 451
Gould, R. J. 1965, Phys. Rev. Lett., 15, 511
Gould, R. J., & Schréder, G. P. 1967, Phys. Rev., 155, 1408
Hacking, P. B., & Soifer, B. T. 1991, ApJ, 367, L49
Halzen, F. 1998, New Astron. Rev., 42, 289
Hara, T., et al. 1993, Nucl. Instrum. Methods A, 332, 300
Harrus, I. M., Hughes, J. P., & Helfand, D. J. 1996, ApJ, 464, L161
Hartman, R. C., et al. 1999, ApJS, in press
Hauser, M. G., et al. 1998, ApJ, 508, 25
Hayashida, N., et al. 1998, ApJ, 504, L71
Hess, M., et al. 1997, in Proc. of the 25th Internat. Cosmic Ray Conf. (Durban, South Africa), ed. M. S. Potgeier, B. C. Raubenheimer, & D. J. van der Walt, 3, 229
Hillas, A. M. 1999, in TeV Astrophysics of Extragalactic Objects, ed. M. Catanese & T. C. Weekes, Astropart. Phys., in press
Hillas, A. M., et al. 1998, ApJ, 503, 744
W. Hofmann 1997, in Proc. Workshop on TeV γ-ray Astrophys. (Kruger Park, South Africa), ed. O.C. de Jager, 405
Hunter, S. D., et al. 1997, ApJ, 481, 205
Hurley, K., et al., 1994, Nature, 372, 652
Jaffe, T. R., et al. 1997, ApJ, 484, L129
de Jager, O. C., & Harding, A. K. 1992, ApJ, 396, 161
de Jager, O. C., & Mastichiadis, A. 1997, ApJ, 482, 874
de Jager, O. C., Stecker, F. W., & Salamon, M. H. 1994, Nature, 369, 294
Jones, T. W., et al. 1998, PASP, 110, 125
Kaaret, P., Piraino, S., Halpern, J., & Eracleous, M. 1999, ApJ, in press (astro-ph/9904249)
Kataoka, J., et al. 1999, ApJ, 514, 138
Kerrick, A. D., et al. 1995a, ApJ, 438, L59
Kerrick, A. D., et al. 1995b, ApJ, 452, 588
Kifune, T., et al. 1995, ApJ, 438, L91
Königl, A. 1981, ApJ, 243, 700
Konopelko, A. 1999, in TeV Astrophysics of Extragalactic Sources, ed. M. Catanese & T. C. Weekes, Astropart. Phys., in press (astro-ph/9901093)
Koyama, M., et al. 1995, Nature, 378, 255
Krennrich, F., et al. 1999, ApJ, 511, 149
Kubo, H., Takahashi, T., Madejski, G., Tashiro, M., Makino, F., Inoue, S., & Takahara, F. 1998, ApJ, 504, 693
Lamb, R. C., & Macomb, D. J. 1997, ApJ, 488, 872
Legage, P. O., & Cesarsky, C. J. 1983, A&A, 118, 223
Lessard, R. W., et al., 1999, in preparation
Lin, Y. C., et al. 1997, ApJ, 476, L11
Macomb, D. J., et al. 1995, ApJ, 449, L99
Macomb, D. J., et al. 1996, ApJ, 459, L111
Madau, P., et al. 1996, MNRAS, 283, 1388
Mannheim, K. 1993, A&A, 269, 67
Mannheim, K. 1998, Science, 279, 684
Maraschi, L., et al. 1999, in TeV Astrophysics of Extragalactic Sources, ed. M. Catanese & T. C. Weekes, Astropart. Phys., in press (astro-ph/9902224)
Maraschi, L., Ghisellini, G., & Celotti, A. 1992, ApJ, 397, L5
Maraschi, L., Ghisellini, G., Tanzi, E. G., & Treves, A. 1986, ApJ, 310, 325
Marscher, A. P., & Travis, J. P. 1996, A&AS, 120, C537
Mastichiadis, A. 1996, A&A, 305, L53
Mastichiadis, A., & de Jager, O. C. 1996, A&A, 311, L5
Maucherat-Joubert, M., Deharveng, J. M., & Cruvellier, P. 1980, A&A, 88, 323
McNaron-Brown, K., et al. 1995, ApJ, 451, 575
Mukherjee, R., et al. 1997, ApJ, 490, 116
Naito, T., & Takahara, F. 1994, J. Phys. G: Nucl. Part. Phys., 20, 477
Neshpor, Y. I., et al. 1998, Astron. Letts., 24, 134
Oliver, S. J., et al. 1997, MNRAS, 289, 471
Ong, R. A. 1998, Physics Reports, 305, 93
Padovani, P., & Giommi, P. 1994, MNRAS, 268, L51
Perlman, E. S., et al. 1996, ApJS, 104, 251
Petry, D., et al. 1996, A&A, 311, L13
Pian, E., et al. 1998, ApJ, 492, L17
Pozzetti, L., Bruzual, A. G., Zamorani, G. 1996, MNRAS, 281, 953
Pozzetti, L., Madau, P., Zamorani, G., Ferguson, H. C., & Bruzual, G. 1998, MNRAS, 298, 1133
Primack, J. R., Bullock, J. S., Somerville, R. S., & MacMinn, D. 1999, in TeV Astrophysics of Extragalactic Sources, ed. M. Catanese & T. C. Weekes, Astropart. Phys., in press (astro-ph/9812399)
Prosch, C., et al. 1996, A&A, 314, 275
Protheroe, R. J., Bhat, C. L., Fleury, P., Lorenz, E., Teshima, M., & Weekes, T. C. 1997, in Proc. of the 25th Internat. Cosmic Ray Conf. (Durban, South Africa), ed. M. S. Potgeier, B. C. Raubenheimer, & D. J. van der Walt, 8, 317
Protheroe, R. J., & Biermann, P. L. 1997, Astropart. Phys., 6, 293
Puget, J.-L., Abergel, A., Bernard, J.-P., Boulanger, F., Burton, W. B., Desert, F.-X., Hartmann, D. 1996, A&A, 308, L5
Punch, M., et al. 1992, Nature, 358, 477
Punch, M. 1997, in Proc. 25th Internat. Cosmic Ray Conf. (Durban, South Africa), eds. M. S. Potgeier, B. C. Raubenheimer, & D. J. van der Walt, 3, 253
Quebert, J., et al. 1995, in Towards a Major Atmospheric Cherenkov Detector - IV (Padova, Italy), ed. M.Cresti, 248
Quinn, J., et al. 1996, ApJ, 456, L83
Quinn, J., et al. 1999, ApJ, in press
Rees, M. J., Phinney, E. S., Begelman, M. C., & Blandford, R. J. 1982, Nature, 297, 17
Reynolds, P. T., et al. 1993, ApJ, 404, 206
Reynolds, S. P. 1996, ApJ, 459, L13
Romani, R. W. 1996, ApJ, 470, 469
Samuelson, F. W., et al. 1998, ApJ, 501, L17
Samuelson, F. W. 1999, Ph.D. thesis, Iowa State University
Schubnell, M. S., et al. 1996, ApJ, 460, 644
Sikora, M., Begelman, M. C., & Rees, M. J. 1994, ApJ, 421, 153
Sinitsyna, V. G., et al. 1997, in Proc. 25th Internat. Cosmic Ray Conf. (Durban, South Africa), ed. M. S. Potgeier, B. C. Raubenheimer, & D. J. van der Walt, 3, 273
Sinnis, G., et al. 1995, Nucl. Phys. B (Proc. Suppl.), 43, 141
Srinivasan, R., et al. 1997, ApJ, 489, 170
Stanev, T., & Franceschini, A. 1998, ApJ, 494, L59
Stecker, F. W. 1999, in TeV Astrophysics of Extragalactic Sources, ed. M. Catanese & T. C. Weekes, Astropart. Phys., in press (astro-ph/9812286)
Stecker, F. W., de Jager, O. C., & Salamon, M. 1992, ApJ, 390, L49
Sturner, S. J., & Dermer, C. D. 1995, A&A, 293, L17
Swanenburg, B. N., et al. 1978, Nature, 275, 298
Swordy, S. P., et al. 1990, ApJ, 349, 625
Takahashi, T., et al. 1994, IAU Circ., No. 5993
Takahashi, T., Madejski, G., & Kubo, H. 1999, in TeV Astrophysics of Extragalactic Sources, ed. M. Catanese & T. C. Weekes, Astropart. Phys., in press (astro-ph/9903099)
Takahashi, T., Tashiro, M., Madejski, G., Kubo, H., Kamae, T., Kataoka, J., Kii, T., Makino, F., Makishima, K., Yamasaki, N. 1996, ApJ, 470, L89
Tanimori, T., et al. 1998a, ApJ, 497, L25
Tanimori, T., et al. 1998b, ApJ, 492, L33
Tavecchio, F., Maraschi, L., & Ghisellini, G. 1998, ApJ, 509, 608
Thompson, D. J., et al. 1993, ApJS, 86, 629
Thompson, D. J., and the EGRET team 1996, private communication
Thompson, D. J., et al. 1995, ApJS, 101, 259
Thompson, D.J. 1997, in Neutron Stars and Pulsars, ed. Shibazaki, N., et al. (Tokyo: Univ. Acad. Press), 273
Toller, G. N. 1983, ApJ, 266, L79
Totani, T. 1998, ApJ, 502, L13

Tümer, T., Bhattacharya, D., Mohideen, U., Rieben, R., Souchkov, V., Tom, H., & Zweerink, J. 1999, in TeV Astrophysics of Extragalactic Sources, ed. M. Catanese & T. C. Weekes, Astropart. Phys., in press
Vacanti, G., et al. 1991, ApJ, 377, 467
Vermeulen, R. C., & Cohen, M. H. 1994, ApJ, 430, 467
von Montigny, C., et al. 1995, ApJ, 440, 525
Weekes, T.C., et al. 1989, ApJ, 342, 379
Weekes, T.C., et al. 1999, VERITAS proposal (http://earth.purdue.physics.edu/veritas)
Weekes, T. C., & Turver, K. E. 1977, in Proc. 12th ESLAB Symp. (Frascati) ESA SP-124, 279
Wurtz, R., Stocke, J. T., & Yee, H. K. C. 1996, ApJS, 103, 109
Yoshikoshi, T., et al. 1997, ApJ, 487, L65
Zweerink, J. A., et al. 1997, ApJ, 490, L141